A REPORT ON

DESIGN AND CONTROL OF ACTIVE ELBOW AND WAIST EXOSKELETON

By

Kartik Joshi

ID: 2019H1060036H

Prepared in partial fulfilment of the

Practice School-II Course No. BITS G639

At

Centre for Artificial Intelligence and Robotics (CAIR), DRDO

Bangalore, India

BIRLA INSTITUTE OF TECHNOLOGY AND SCIENCE, PILANI
(Hyderabad Campus)

Jan 2021 -June 2021

ACKNOWLEDGEMENT

This project has been a great learning for me. Apart from giving an opportunity to learn and work on one of the cutting-edge sciences in the World, it has also provided invaluable research experience which is more than what M. Tech students can hope for.

It would be impossible to do justice in thanking Dr. Shubhashisa Sahoo using mere words, but I would like to make an attempt. Dr. Shubhashisa Sahoo is not only a guide but also an inspiration to all of us. His guidance at every step of the project was crucial to us. During my time at Intelligent Systems and Robotics Division in the Centre for Artificial Intelligence and Robotics DRDO, his continued insistence to hold us in good stead in the years to come.

I take this opportunity to thank Dr Desiraju Padma, Head of the Intelligent Systems and Robotics Division, CAIR.

I wish to thank Dr Upendra Kumar Singh, Director of the Centre for Artificial Intelligence and Robotics, for giving us the opportunity to work at the Intelligent Systems and Robotics Division.

I take this opportunity to thank Mr S. Raghuraman, practice school (PS) guide, BITS Hyderabad, for his inputs and advice at every step of the project.

I am grateful to Mr Pradeep Sharma, a Technical Assistant in CAIR, for his constant assistance in learning new software's and installations of the same on time to time.

I am thankful to Krishnadev, Prathmesh, Joji, Debashish, Akshay, Suchithra, Debanjali, and Rudra for being my friends, always ready to help in their own way.

If I have forgotten to mention I sincerely apologize. I am grateful to everyone who helped me throughout the course, my work and the production of this thesis.

Practice School Division

Station Name: CENTRE FOR ARTIFICIAL INTELLIGENCE AND ROBOTICS (CAIR),DRDO

Centre: Bangalore **Duration:** 6 months

Date of Start: 12th Jan 2021 **Date of Report Submission:** 7h June 2021

Title of the Project: Design and Control of Elbow joint and Lumbar/Waist Joint Exoskeleton

Name: Kartik Joshi **ID No:** 2019H1060036H

Discipline of Student: Mechanical Engineering

Name and Designation of the Expert: Dr. Subhashisa Sahoo, Scientist

Name of the PS Faculty: Prof. S. Raghuraman

Project Areas: Robotics, Control System

ABSTRACT

Keywords: Assistive Devices, Biomedical Engineering, Upper Limb Exoskeletons, Inertial Measurement Units (IMU), Wearable Robotics Devices, OpenSim

We know that individual safety is a significant aspect of daily life, probably even more so in the defence army.

Active soldiers normally have to carry heavy loads during missions, which puts pressure on their upper arms, backs, hips etc. Excessive load over long duration may cause fatigue-based injuries which can be detrimental to the soldier's health and the missions success. Therefore, the defence research must come up with new technologies that allow to alleviate the joint stresses by augmenting the strength of the wearer. In this project, our goal is to develop exoskeleton for assisting the motion of the wearer.

We have studied the motion capture data of 100 soldiers carrying different weights in hands and walking with different speeds. The simulation is performed in Opensim software to perform inverse dynamics in order to determine out joint reactions, forces, moments etc.

The actuators and gear ratio for exoskeleton are selected based on maximum moments and joint velocity (elbow, lumbar/waist joints). This information is used to determine feasible alternatives for the motor and gear ratios.

The control system for the exoskeleton is designed so that the exoskeleton is able to efficiently track and provide assistance to the wearer. Input for the controller is collected from IMU,pressure sensors and motor encoders in the current study. Ideally the exoskeleton must be able to track the joint perfectly and instantly, however that is not practically realizable due to numerous unavoidable reasons thus the aim is to reduce the settling time and error.

Signature of student
Date:

Signature of PS faculty
Date:

BIRLA INSTITUTE OF TECHNOLOGY AND SCIENCE, PILANI
(Hyderabad Campus)
Practice School Division

Response Option Sheet

Station: Centre for Artificial Intelligence and Robotics (CAIR), DRDO

Centre: Bangalore

Name : Kartik Joshi **ID No.:** 2019H1060036H

Title of the Project: Design and Control of Elbow and Lumbar/Waist Exoskeleton

Code No.	Response Options	Course No. & Name
1.	A new course can be designed out of this project	NA
2.	The project can help modification of the course content of some of the existing courses.	NA
3.	The project can be used directly in some of the existing Compulsory Discipline courses (CDC) /Disciplines Compulsory Discipline courses (DCOC) / Emerging Area (EA) etc. Courses	NA
4.	The project can be used in preparatory courses like Analysis and Application Oriented Courses (AAOC)/ Engineering Science (ES)/ Technical Art (TA) and Core Courses.	NA
5.	This project cannot come under any of the above-mentioned options as it relates to the professional work of the host organization.	**Applicable**

Signature of student
Date:

Signature of PS faculty
Date:

INDEX

LIST OF TABLES

LIST OF FIGURES

	(g) TRACKING RESPONSE : 29 Kg (h) TORQUE PROFILE: 29 Kg TRACKING AND TORQUE OF ELBOW EXOSKELETON IN PRESENCE OF DISTURBANCE	
17	(a) TRACKING RESPONSE : NO LOAD (b) TORQUE PROFILE: NO LOAD (c) TRACKING RESPONSE : 17 Kg (d) TORQUE PROFILE: 17 Kg (e) TRACKING RESPONSE : 22.6 Kg (f) TORQUE PROFILE: 22.6 Kg (g) TRACKING RESPONSE : 29 Kg (h) TORQUE PROFILE: 29 Kg TRACKING AND TORQUE OF LUMBAR/WAIST EXOSKELETON IN ABSENCE OF DISTURBANCE	72-73
18	(a) TRACKING RESPONSE : NO LOAD (b) TORQUE PROFILE: NO LOAD (c) TRACKING RESPONSE : 17 Kg (d) TORQUE PROFILE: 17 Kg (e) TRACKING RESPONSE : 22.6 Kg (f) TORQUE PROFILE: 22.6 Kg (g) TRACKING RESPONSE : 29 Kg (h) TORQUE PROFILE: 29 Kg TRACKING AND TORQUE OF LUMBAR/WAIST EXOSKELETON IN PRESENCE OF DISTURBANCE	74-75

CHAPTER 1

1.1. INTRODUCTION

Exoskeletons are devices that is worn by a user and works in tandem in order to provide assistance, decrease effort and increase strength. Exoskeleton was created to help workers in automotive, construction, etc. The use of exoskeleton is able to reduce fatigue and injuries thereby increasing overall productivity.

The exoskeletons can be both active and passive depending if the support/assistance is provided using an actuator or with the help of springs. Active exoskeletons are more complicated than passive exoskeletons as they require controllers, actuators, battery's, etc. Active exoskeletons however have an advantage over passive exoskeletons despite their complex design as they allow for assistance as needed depending on the load and can provide a constant ratio of supporting torque which is more similar to what the wearer will feel without the exoskeleton. This allows for smoother and less restricted movement which also reduces the learning curve and the chance for injuries.

Exoskeletons can be made up of soft and flexible material or rigid links. They both have their own advantages however rigid link exoskeletons are more common to simplicity of design and better load bearing and range of motion capabilities.

Exoskeleton has found application in medical rehabilitation for patients who have lost the function of their limbs partially or completely and in defence as a support and combat tool. In defence the aim is to primarily augment the strength of the wearer to allow for higher repetition for a given load/task and increase the overall strength of the wearer allowing them to carry heavier weights for longer distances. It has the potential to significantly improve the success rate for army's tactical missions allowing for heavier payload to be carried. It can also be advantageous in hand-to-hand combat scenarios where strength of the user can play a major factor.

1.2. HISTORY

The earliest mention of a device resembling an exoskeleton was Yang's running aid in 1890 [1]. It was a passive device with bow–spring. It was intended to augment running speed and jumping height of the wearer.

In 1917 Leslie C. Kelley in US developed a machine which uses steam to power artificial ligaments arranged in parallel to the wearer's movements thus augmenting their strength [2].

Around 1965 the US Naval research funded General Electric to develop the first full-body active exoskeleton model that can drastically augment wearers strength. The robot was name 'Hardiman' [3]. It was hydraulically powered, weighing around 680Kg with 30 DOF. It could augment the strength of

the user allowing them to lift weight 25 times their capability. The project however was overall unsuccessful due to uncontrolled and violent motion of limbs.

In 1969 active exoskeletons were being researched and developed at the Mihajlo Pupin Institute [4]. It was a 4 DOF lower limb exoskeleton which was electrically actuated by DC motors. The purpose of the robot was to be used as a rehabilitation tool for paraplegic patients.

In 1997 Hybrid Assistance Robot (HAL) [5] was being developed in Tsukuba University, Japan. The 5th version of HAL was finished in the year 2012 which is a full body exoskeleton. HAL was designed with the purpose of augment the strength of the wearer and assist the elderly in their daily tasks.

BLEEX [6], a 7 DOF (4 powered) lower limb exoskeleton developed in 2006 as the most prominent Defence Advanced Research Projects Agency (DARPA) project. BLEEX used hydraulic actuators and was aimed at significantly augmenting the wearers strength.

There have been many exoskeletons over the years pushing forward the research and development for applications ranging from strength augmentation to rehabilitation of limbs. Some of the most advance exoskeletons available include SIAT-WEXv2 [7], Harmony [8], etc.

1.3. LITERATURE REVIEW

In this section a brief discussion on existing exoskeleton models is presented to give an overview of the various technologies being used, their advantages, disadvantages and implementation.

The exoskeletons can be categorised based on their application ass medical rehabilitation, assistance and strength augmentation.

Hardiman [3] was one of the first powered exoskeleton to be developed. It was a 30 DOF full body exoskeleton based on master and slave control. It had an inner slave exoskeleton whose movement was to be mimicked by the master exoskeleton. The project was aimed at augmenting the strength of the user and was a project funded by Défense Advanced Research Project Agency (DARPA) for military applications. The exoskeleton used hydraulic actuators and position control strategy. The project was deemed unsuccessful due to violent uncontrolled behaviour of the exoskeleton.

Mihajlo Pupin Exoskeleton [4] was one of the earliest active exoskeletons. It was developed in Yugoslavia around the time of development of Hardiman. It is a lower body exoskeleton aimed at providing medical assistance. It is a 4 DOF active exoskeleton that uses pneumatic actuator. The control strategy used by it is Zero Moment Point (ZMP). In this control methodology the moment about the centre of the sole of two feet is taken as zero and during walking phase when only one leg contacts the ground is taken as the centre of the sole of that foot. This control method allows for dynamic stability of the exoskeleton during walking.

BLEEX [6] exoskeleton was developed in 2006 and also aimed at augmenting the strength of the wearer. It is a 7 DOF (each leg) lower body exoskeleton, 3 of the 7 DOF were active and powered using hydraulic actuators. It used Hybrid control strategy employing position and Sensitivity Amplification

Control (SAC) to control the movement of the joints. It also used dynamic model to predict the joint torque which was fed as the joint input torque. The dynamic model needs to be highly accurate for this type of control.

H-WEX [15] was developed by Hyundai in 2017 and weighs 4.5 Kg. It is a lumbar/waist exoskeleton with 2 active DOF (1 at each hip joint in sagittal plane for flexion and extension). It used BLDC motors and a cable driven system. The cable driven system ensured that the motion of the joint was not restricted. It used IMU sensors and encoders to gather joint information. It used torque control in order to control the exoskeleton.

CAREX-7 [13] is a 7 DOF (3 at shoulder, 1 at elbow, 1at wrist) arm exoskeleton developed in 2012. It weighs in as 1.55 Kg and uses series elastic actuators (uses a spring cable arrangement with motor) for better compliance with the environment. The end-effector force was measured using a load cell. It uses 2 level of control, high-level wrench field controller and a low-level cable-tension controller (PI controller).

NEURO-Exos elbow module[18] is a 1 DOF active elbow exoskeleton. It uses series elastic actuator using Maxon EC60 motor with harmonic drive of 1:80 gear ratio. It uses encoders to determine joint position. It uses two level controller, high level controller (implements warm up routine and set of pre-determined rehabilitation tasks) and a low-level position and torque controller.

A brief description about various robot and their specification is mentioned in TABLE 1 which is used as a reference for better understanding the design and controller used in the exoskeleton.

TABLE 1 : LIST OF EXOSKELETONS AND THEIR SPECIFICCATIONS

S.No.	NAME	APPLICATION	SUPPORTED MOVEMENT	DEGREE OF FREEDOM (DOF)	ACTUATOR	MOTION DATA COLLECTON	CONTROL STRATEGY	WEIGHT (Kg)
1	ABLE[9]	Medical Rehabilitation and assistance	Shoulder (FE, AA, IE), Elbow (FE)	4-Active (Each Arm)	DC Faulhaber type motor Screw-cable transmission	-	Force feedback control	8
2	APO[10]	Medical Rehabilitation	Hip (FE, AA)	1-Active 1-Passive (Each Leg)	SEA (Maxon EC 60 with incremental encoder)	Encoders	Adaptive oscillator–based control (high level) Torque control (low level)	4.2
3	Atalante[12]	Medical Rehabilitation	Hip (FE, AA, IE), Knee (FE), Ankle (FE, AA)	6-Active (Each Leg)	BLDC Motor	Encoders, IMU sensors, 3-axis force sensors	Hybrid Control	-
4	BLEEX[6]	Strength Enhancement	Hip (FE, AA, IE), Knee (FE),	3-Active 4-Passive (Each Leg)	Hydraulic	Encoders, Linear accelerometer	Hybrid Control	14

			Ankle (FE, AA, rotation)				(Position control & Sensitivity Amplification Control)	
5	BONES[11]	Medical Rehabilitation	Shoulder (EF, AA, rotation), Elbow (EF)	4-Active (Each Arm)	Pneumatic	Encoders	Force control	-
6	CAREX-7[13]	Assistance	Shoulder (EF, AA, rotation), Elbow (EF), wrist (EF, AA, pronation-supination),	7-Active (Each Arm)	servomotors (Kollmorgen AKM™ Series) Cable driven	IMU sensors	High level wrench-field controller Low-level cable-tension controller (PI controller)	1.55
7	Hardiman[3]	Strength Enhancement	Full Body Exoskeleton	30	Hydraulic Electric Motor (Valve control)	-	Master and Slave Control; Position control (tickler method)	680
8	HAL 5[14]	Medical Rehabilitation and assistance Strength Enhancement	Hip (FE), Knee (FE), Shoulder (EF), Elbow (EF) (FULL BODY)	4-Active (Each Limb)	DC Motor	Bioelectrical sensors (EMG), IMU sensors, Angular sensors, Acceleration sensors, Force sensors (COP/COG sensors)	Hybrid Control System (Cybernic Voluntary Control, Cybernic Autonomous Control)	23
9	H-WEX[15]	-	Hip (FE, AA) – one dimensional support (WAIST EXOSKELETON)	2-Active 2-Passive	BLDC Motor with harmonic drive Cable driven	IMU sensors, Encoders	Torque Control (Assist mode & walking mode)	4.5
10	LOPES[16]	Medical Rehabilitation	Hip (FE, AA), Knee (FE) Guides (Left/Right, Forward/Backward)	5-Active (3 in exoskeleton -Each Leg; 2 in guides)	SEA [Servomotor (Kollmorgen AKM22C)-EXOSKELETON with Neugart Planetary Gear (64:1) servomotors (Berger Lahr SER3910)-GUIDE with Neugart Planetary Gear (64:1)]	LVDT Sensor	Impedance Control	-
11	Mihajlo Pupin Exoskeleton[4]	Medical assistance	Hip (FE, AA), Knee (FE) Ankle (FE)	4-Active (Each Leg)	Pneumatic	Pressure Sensor	ZMP control	12 (power source and computer control-not

								located in the device)
12	National University of Singapore Exoskeleton[17]	Strength Enhancement	Hip (FE), Knee (FE), Ankle (FE)	3-Active 3-Passive	SEA (Maxon BLDC motor)	Encoders	Locomotion Control ZMP control	34.56
13	NEURO-Exos elbow module[18]	Medical Rehabilitation and assistance	Elbow (FE)	1-Active	SEA (Maxon EC60 with harmonic drive of 1:80 gear ratio)	Encoders	Two Layer control- High Level Control- implements a warm-up routine and a set of pre-defined rehabilitation exercises Low Level Position Control and Torque Control	-
14	Powered Hip Exoskeleton for Walking Assistance (PH-EXOS)[19]	Medical Rehabilitation and assistance	Hip (FE) (Each Leg)	1-Active 2-Passive	YASKAWA servo AC motor (SGMAH-01AAA41) with 40:1 gear ratio Flexible Bowden cable transmission systems	Angular displacement potentiometer (WDJ22A) 4 FRS sensors (FlexiForce-A301)	Cascade PID control Fuzzy adaptive logic control (Both implemented and compared)	3.5
15	SIAT-WEXv2[20]	Strength Enhancement	Waist (FE)	1-Active	BLDC Motor (Maxon EC90) with Harmonic Drive	Encoder IMU sensors	Fuzzy adaptive control	4.9
16	Soft Exosuit for Hip Assistance (Harvard University) by Alan T. Asbecka, Kai Schmidta, Conor J. Walsha[21]	Assistance	Hip (FE)	1-Active (soft design)	Maxon EC30 with gear box of 1:23 gear ratio	Encoder	Position Control	7.57
17	Upper Limb Exoskeleton by Borhan Beigzadeh, Mahdi Ilami and Sohrab Najafian[22]	Assistance	Elbow (EF)	1-Active	DC Motor	IMU sensor EMG Sensor (separate test as control input)	Admittance Control	-
18	VariLeg[23]	Medical Rehabilitation and assistance	Hip (FE, AA), Knee (FE)	3-Active	Variable Stiffness Actuator (VSA) (Maxon EC90 with harmonic drive and 1:160 gear ratio)	IMU sensor	High Level Control (trajectory calculation) Low Level Position Control	-

1.4. STATE OF THE ART

The exoskeleton is an emerging field with massive potential for application in rehabilitation, prosthetic, strength augmentation for military and industrial purposes. There has been increased research and progress in novel design and control of exoskeleton in recent years. The level of technology is still in budding phase but is still being widely accepted and used for industrial, military and medical applications.

There is no set standard prescribed to measure the performance of exoskeleton, however metabolic cost is most widely used. Very few studies have shown to significantly reduce the metabolic cost associated with a task. It is very difficult to quantify assistive exoskeletons as the metric of importance in such cases is fatigue, strength, repetition, etc.

Most of the control methods are focused on users of joint motion or joint torque. A common approach for safe human-robot interaction is the use admittance controller or impedance controller. The interaction forces in these controllers are controlled via a mass-spring-damper system [29].

In strength augmentation applications through exoskeleton requires additional joint torques depending upon the load begin moved. The user movement and the required joint torques can be obtained through either by measuring the force/torques directly through force sensors at human-exoskeleton interface or with the help of EMG sensors to sense the electrical activity in the muscles when lifting a load [31].

Some of the state-of-the-art research in the field of exoskeleton robot is being conducted around the usage of EMG sensors, control systems and soft robotics. Surface EMG sensors are being used to determine and predict the motion of the joints and the force generated by the muscles before the actual movement of the joint, this however has proven to be difficult as seen from HAL [14] robot as it is difficult to standardize, thus needs to be calibrated for each user.

There are various ways to correlate the muscle activity in terms of EMG signals to joint toques like biomechanical models [31][32], proportional mapping model [33][34] or machine learning algorithms [35].

Control system play a vital role in the performance of the exoskeleton and needs to have very fast response and settling time. The current research using adaptive control strategy uses neural network to change the parameters in order to ensure that the robot performs well even in drastically varying conditions.

The control system algorithm which is based on force and/or EMG signals to provides assistance to the user depending upon the assistance needed to move the arms is known as assistance as needed

(AAN) and is widely being researched [28]. AAN control strategy was used by BLEEX [6] exoskeleton employing model-based approach to determine joint torques as a relation to joint positions.

There is also a need to research and design actuators that are smaller, lighter and more efficient thus alternate actuation mediums such as shape memory alloys (eg. Nitinol) is being researched. Soft robotics is another field of research emerging as a sub-category for exoskeletons that uses soft and flexible materials and/or design for exoskeleton limbs. An example of flexible robot involves the use of artificial muscles (there are many different designs one such is the flexible braided tubes using compressed air for actuation).

CHAPTER 2

2.1 INTRODUCTION

Exoskeleton robots ideally are an extension of the human limbs and must mimic the motion in order to provide assistance and/or enhance strength. The study of human joints allow for a better understanding of what joints are causing motion and the degree to which they move when a given task is performed. This information is of high importance in deciding the degree of freedom (DOF) of the robotic links.

If unnecessarily more DOF is provided to a joint that would just complicate the design, increase the weight and not add any value. If the DOF is less than what is required then it may either restrict the motion causing discomfort or additional strain which is counter intuitive or not provide adequate assistance for some tasks.

The study of joints allows for choosing the right DOF so that the motion is not restricted and the assistance is provided in the plane where it is most requires, for example it may not be useful to provide assistance laterally to the shoulder if it is to be designed for a specific task where the movement of the shoulder is primarily that of flexion/extension.

After deciding upon the joint range of motion and DOF for the exoskeleton it is important to study the joint velocities, acceleration and moment. This information is useful in selection of the actuators and gear ratio (if needed). If the actuator selection is improper then the exoskeleton may not be able to properly track the joint and provide assistance. The actuator selected should be such that its capabilities lie well within the task requirements (choosing a factor of safety (FOS) depending how dynamic is the task)

2.2 HUMAN ANATOMY

The study and movement of human joints are important for selection of DOF for the robotic exoskeleton. The human body is segmented with imaginary planes that is used to better classify and understand the joint motion.

A. PLANES

The human body is segmented into 3 mutually perpendicular planes and is done in order to differentiate the movement of the joints across these planes.

The 3 planes are-

- **<u>Sagittal Plane</u>**

  It is the plane that divides the body into left and right half. Motion in this plane is important for advancing the body forward

❖ **Coronal Plane**

It is a plane that is perpendicular to sagittal and transverse plane and divides the body into ventral (stomach side) and dorsal (back side) section

❖ **Transverse Plane**

It is a plane that is perpendicular to Sagittal and Coronal planes and divides the body horizontally into superior (upper half) and inferior section (lower half).

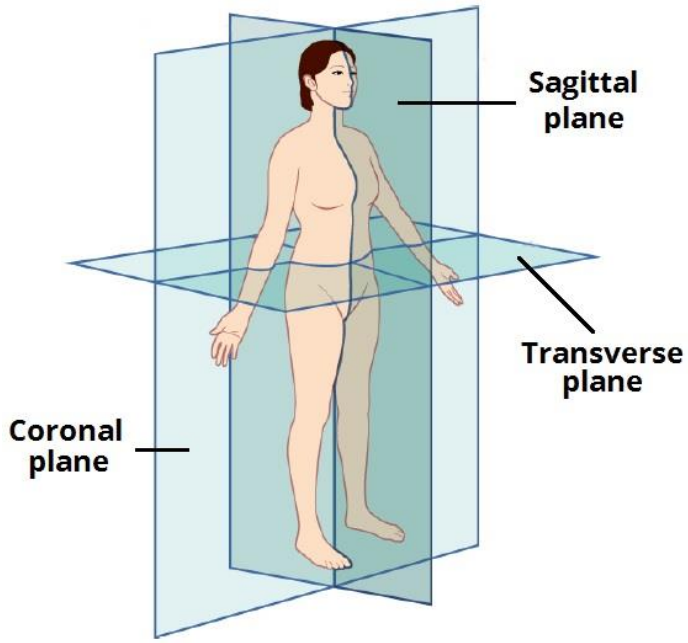

Fig. 1 : ANATOMICAL PLANES OF HUMAN BODY

(By Connexions (http://cnx.org) [CC-BY-3.0]**)**

B. JOINTS

The human body has numerous simple and complex set of joints that allow different motions possible. Each joint has a set DOF and a range of motion up to which it can move.

The joints can be classified based of the amount of movement as-

❖ **Synarthrosis**

- Permits little or no mobility
- They are mostly fibrous joints (joints connected by fibrous tissue)

❖ **Amphiarthrosis**

- Permits very little mobility
- They are mostly cartilaginous joints (joints connected by cartilage)

❖ **Synovial**

- They are freely moveable
- They are further subdivided into 6 groups based on the type of movement they permit-
  - ➢ Plane joint

- Ball and socket joint
- Hinge joint
- Pivot joint
- Condyloid joint
- Saddle joint

The focus of the study will be kept on synovial joints as they provide large movement and contribute the most towards the movement of the limbs as opposed to synarthrosis and amphiarthrosis joints that contribute little to none.

The aim of the study is to design a robotic exoskeleton for elbow joint and lumbar joint hence only these joints along with hip joint are mentioned and studied in detail as they are directly important to the current study.

- **LUMBAR/VERTEBRAE-**

  There are 24 vertebrae in an adult human spine (babies are born with 33, 9 of which are fused together as we get older) that are connected and interact with each other through the joint known as facets.

  The vertebrae are divided into 5 segments-

  - Lumbar Spine - It consists of 5 vertebrae from L1 to L5 in the lower back
  - Thoracic Spice - It consists of 12 vertebrae from T1 to T12 in the mid back
  - Cervix Spine- It consists of 7 vertebrae fromC1 to C7 in the mid back
  - Sacrum – It consists of 5 fused vertebrae
  - Causal – It consist of 4 fused vertebrae

  The maximum motion of the back during bending down, walking or other daily tasks occurs at the lumbar spine segment (L1 to L5 vertebrae). During the design phase for a lumbar exoskeleton, it has to ensure that the motion is not restricted particularly in this lumbar spine. The exoskeleton can be designed using either with a flexible joint, one such commonly used solution is scissor mechanism. The other solution for waist portion of the exoskeleton is by using a rigid link but it is offset so as to provide enough room to account for the lumbar bending. Soft exoskeleton is also a viable solution as they do not tend to restrict movement.

  The hinged motion in the sagittal plane about lumbosacral joint is of primary concern while designing the waist/lumbar exoskeleton as the assistance is to be provided to the robot in the sagittal plane as large motion occurs only about this plane for majority of the tasks such as bending and lifting, walking, etc.

- **Lumbosacral joint**

  It is a synovial joint formed by articulation between the L5 vertebrae and the sacrum (S1) (They articulate at an angle of 140̊) as well as two lumbosacral facet joints (right and left zygapophysial joints)

  Movement of the Lumbosacral joint –

  - **Flexion -** Ventral movement of torso in the sagittal plane
  - **Extension -** Dorsal movement of torso in the sagittal plane
  - **Lateral Flexion –** Lateral or side to side movement of the torso (coronal plane)

❖ **HIP –**

It is a synovial ball and socket joint formed by the interaction between pelvic acetabulum (socket) and the head of the femur (ball). The cavity of the socket is deeper due to the presence of a fibrocartilaginous collar – the acetabular labrum. It is designed for stability and bearing weight rather than for a large range of motion.

Movement of the joint-

- **Flexion –** This movement draws the thigh towards the trunk (in sagittal plane)
- **Extension** - This movement draws the thigh away from the trunk (in sagittal plane)
- **Abduction -** Movement of the thigh in the coronal plane away from the mid-plane (sagittal plane)
- **Adduction -** Movement of the thigh in the coronal plane towards from the mid-plane (sagittal plane)
- **Internal Rotation –** The femoral shaft moves anteriorly, causing the toes to point medially
- **External Rotation -** The femoral shaft moves posteriorly, causing the toes to point away from mid-line

❖ **ELBOW –**

It is a compound joint that is formed by the articulations of 2 surfaces, distal end of the humerus of the upper arm and the proximal end of radius and ulna bones in the forearm.
The hinge motion of the joint is due to humeroulnar and humeroradial joint and is limited to about 180̊ by the olecranon at the distal end of the ulna (bulge of the bone).
The pronation and supination of the joint is due to the pivot motion of the radioulnar joint. The pronation is limited due to radial bone crossing over ulna while supination is limited due to tension in the ligaments

- **Humeroulnar joint**

  It is a synovial hinge joint formed between trochlea on the medial aspect of the distal end of the humerus and the trochlear notch on the proximal ulna.

- **Humeroradial joint**

  It is a synovial hinge joint formed between capitulum on the lateral aspect of the distal end of the humerus with the head of the radius.

- **Radioulnar joint**

  It is a synovial pivot joint formed between proximal ends of the radial and ulna.

  Movement of the elbow joint-

  - **Flexion -** Decreasing the angle formed between upper arm and the forearm
  - **Extension -** Increasing the angle formed between upper arm and the forearm
  - **Pronation –** Turning the forearm (at the elbow) such that the palm of the hand is facing upwards
  - **Supination -** Turning the forearm (at the elbow) such that the palm of the hand is facing downwards

C. JOINT LENGTH, MASS, CENTRE OF MASS AND MOMENT OF INERTIA

The joint length, mass and centre of mass of the body is an important parameter while designing an exoskeleton robot. Joint length gives information about the link lengths to be used for the exoskeleton robot.

Location of link length, mass and centre of mass are important parameters that are used to find the dynamics equation of the human body.

The join lengths and mass are found to vary proportionally with the height of the person, that is the limbs of a person who is taller tend to longer and heavier which is also roughly in the same proportion to the length of the whole body as found by De Leva[24].

In De Leva's paper the subject's height were 174 cm and weight was 73 Kg for men's. The Indian average of height and weight for men is different from in the study but its conclusion that the percentage ratio remains the same is used to find the joint lengths, mass and centre of mass for the Indian average height that is of primary concern in this study.

The average weight o Indian man is 65 Kg and the average height is about 165 cm and from here on all discussion is considered pertaining to these values.

In TABLE 2 the percentage ratio of the body parts/segments with total weight (65 Kg) and total height (165cm) for Indian average is compiled

TABLE 2 : LIST OF BODY PARTS WEIGHT AND LENGTH

S.No.	BODY PART/ SEGMENT	PERCENTAGE OF TOTAL WEIGHT	WEIGHT IN Kg (CONSIDERING 65Kg TOTAL WEIGHT)	PERCENTAGE OF SUBJECT HEIGHT	LENGTH IN cm (CONSIDERING 165 cm SUBJECT HEIGHT)
1	HEAD	6.94	4.511	13.95939	23.033
2	TRUNK	43.46	28.249	36.7575	57.56
3	UPPER ARM	2.71	1.7615	14.06848	23.213
4	FOREARM	1.62	1.053	14.44242	23.83
5	HAND	0.61	0.3965	10.8563	17.9129

In TABLE 3 the percentage ratio of the body parts/segments with the length of the joint for defining the location of the centre of mass with respect to the proximal end of the body part/segment. It also complied information regarding Moment of Inertia which is useful in later chapters where this information is taken as parameter values for the human body's kinematic and dynamic equations.

TABLE 3 : LIST OF BODY PARTS AND THEIR LOCATION OF CENTRE OF MASS

S.No.	BODY PART/ SEGMENT	CENTRE OF MASS AS % OF BODY PART/SEGMENT FROM PROXIMAL TO DISTAL END (IN SAGITTAL PLANE)	CENTRE OF MASS IN cm FROM PROXIMAL TO DISTAL END CONSIDERING 165 cm AS TOTAL HEIGHT (IN SAGITTAL PLANE)	MOMENT OF INERTIA ABOUT CENTROID (z-axis, perpendicular to sagittal plane)
1	HEAD	59.76	13.7645208	0.009179488483
2	TRUNK	44.86	25.821416	2.254287152
3	UPPER ARM	57.72	13.3985436	0.0005465727083
4	FOREARM	45.74	10.899842	0.0001167575877
5	HAND	36.91	6.61165139	0.000006233465713

From the information given in TABLE 2 and TABLE 3 the mass, location of centre of mass and Moment of Inertia is found that is useful for designing and control of lumbar/waist and elbow exoskeleton.

The lumbar/waist exoskeleton carries the entire upper body whose mass is 39.18 Kg and the location of centre of mass for the upper body in sagittal plane is 31.31 cm (considering all the joint angles as zero, i.e., perfectly straight posture) from the lumbar joint (It varies with the angle of elbow and shoulder but since their mass is very less in comparison to torso thus is neglected).

Similarly for elbow exoskeleton the centre of mass is located at 17.3659 cm from the elbow joint with a total mass of 1.4495 Kg.

D. ROBOT DESIGN

The robot design can be split into 2 parts, one is the selection of materials for links and the other is the kinematic arrangements of link and location of the electronics. This division is made is interdependent to some extent depending upon the targeted capacity of assistance of robot, application, etc.

The material preferred for use in exoskeleton are usually those with very high specific strength except in case of soft robotics. Some of the commonly used materials for exoskeleton include carbon fibre, aluminium alloys, etc. Sometimes titanium alloys may also be used if there are large loads that the exoskeleton has to assist.

The lumbar/waist exoskeleton is chosen to be made of rigid link with offset as the exoskeleton is to be designed for defence application thus has to be sturdy, reliable and be capable of providing large amount of assistance which is easier if there are fewer moving parts and a frame is strong and rigid.

It is important to ensure that the motion of the spine about the coronal and transverse plane is not restricted by lumbar/waist exoskeleton as it may cause the wearer difficulty in walking and maintaining balance which would be counterintuitive as the exoskeleton aims at augmenting strength for defence applications.

The lumbar/waist exoskeleton is strapped onto the thighs and waist thus it is also important to ensure that the hip movement is not restricted. The twisting and lateral movement of the torso about the lumbar spine is minimum thus it is preferred that the end effector of the lumbar /waist link is in that region as this will simplify the problem so that it automatically accounts for asymmetrical lifting since the movement about coronal and transverse plane is minimal and can be neglected. However, it will not pose any significant issues even if the lumbar link is long and strapped onto shoulders (easier anchor point).

The elbow exoskeleton design is simple with a single rigid link across the length of the forearm providing assistance in the sagittal plane (flexion/extension). A 1 DOF exoskeleton providing assistance for both flexion/extension and pronation/supination is not chosen as the fatigue due to pronation/supination is not the limiting factor. Single rigid link should be designed such that it does not restrict pronation/supination as it may cause pain the in the bones due to shear stress acting on them. One way is to have a separate passive DOF to account for pronation/supination.

It is preferred that the link is wider at the point of interface with the human so that there is not a lot of pressure acting on the skin to cause discomfort or damage.

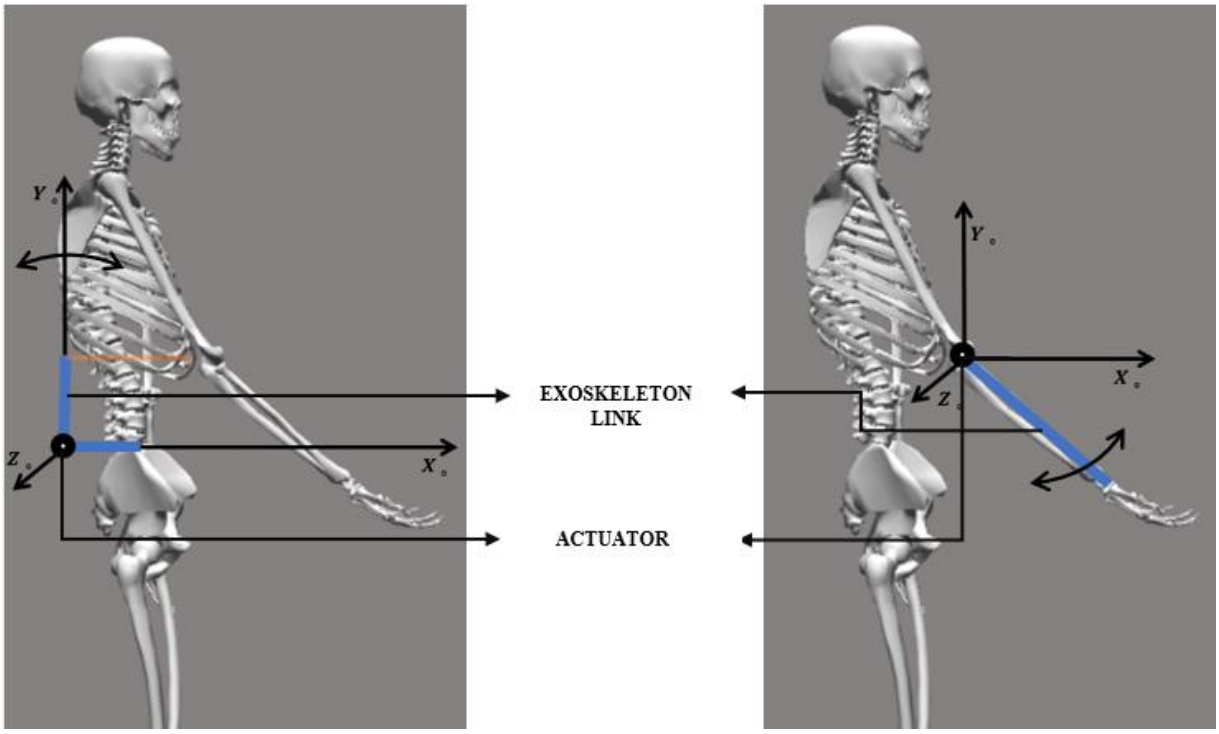

(a) (b)

Fig. 2 (a) REPRESENTATION OF LUMBAR/WAIST EXOSKELETON (b) REPRESENTATION OF ELBOW EXOSKELETON

In the current study the material chosen for the elbow and lumbar/waist exoskeleton is carbon fiber which has a density of 2 gm/cm^3. The mass of the link is roughly about 4.6 gm if a solid link of 3 cm in diameter is selected which is extremely less and can be neglected. Adjusting for additional equipments such as sensors, straps, etc. the total mass of the exoskeleton is about 1.5 Kg (excluding the motor). This mass value is realistic as seen from survey of journals,confereces,etc.

Similarly for lumbar/waist exoskeleton the estimated mass is about 2 Kg. Mass of lumbar exoskeleton is slightly more since the link needed and straps required to anchor will be lnger and wider as it has to provide much higher values of torque as opposed to elbow exoskeleton.

The centre of mass is assumed at the centre of the link for both the lumbar/waist and elbow exoskeleton.

2.3 EXPERIMENTAL GAIT DATA

The experimental data was collected to using X-sense motion capture with 17 markers (IMU sensors) placed on the body of the test subject that was assigned a task to capture joint motion, velocity and acceleration. The test was conducted as a combined effort from DBEL and CAIR to realize upper body exoskeleton. The experiment was performed for 100 army soldiers with an average wight of about 65 Kg.

The experimental data collected was fed into AnyBody software which user complex mathematical model to find joint reaction, muscle forces, muscle activation, power requirement, etc. The results from

AnyBody were also verified using OpenSim which is an open-source software. There were slight discrepancies as expected due to the use of different solvers and different body models.

The aim of conducing this experiment is to test the working limits of the exoskeleton based on which battery and motors can be selected. This is of great importance as battery is the heaviest component in the exoskeleton, thus actuator selection is of prime importance so that it does not consume unnecessary power and there is need for a larger and heavier battery. Increased weight of exoskeleton negatively impacts its performance.

The experimental data collected can also be used to determine what is the percentage of reduced muscle activation which can be a sign of reduced metabolic cost.

A. TASK ASSIGNED

The soldiers were assigned a task to walk up to a box, bend-down and pick up the box and walk with the box. The test was conducted for 3 different box weight – 17 Kg, 22.6 Kg and 29 Kg. In addition to this for each weight the test was further classified as normal walk (NW) and fast walk (FW) where the soldiers were instructed to walk at normal pace or fast pace. For 29 Kg box weight fast walk test was not conducted as the weight of the box was very heavy.

Each test was repeated 2 times to ensure consistency. Thus, the total number of tests for each soldier was 5 which were repeated times that is each soldier was part of the 10 trials.

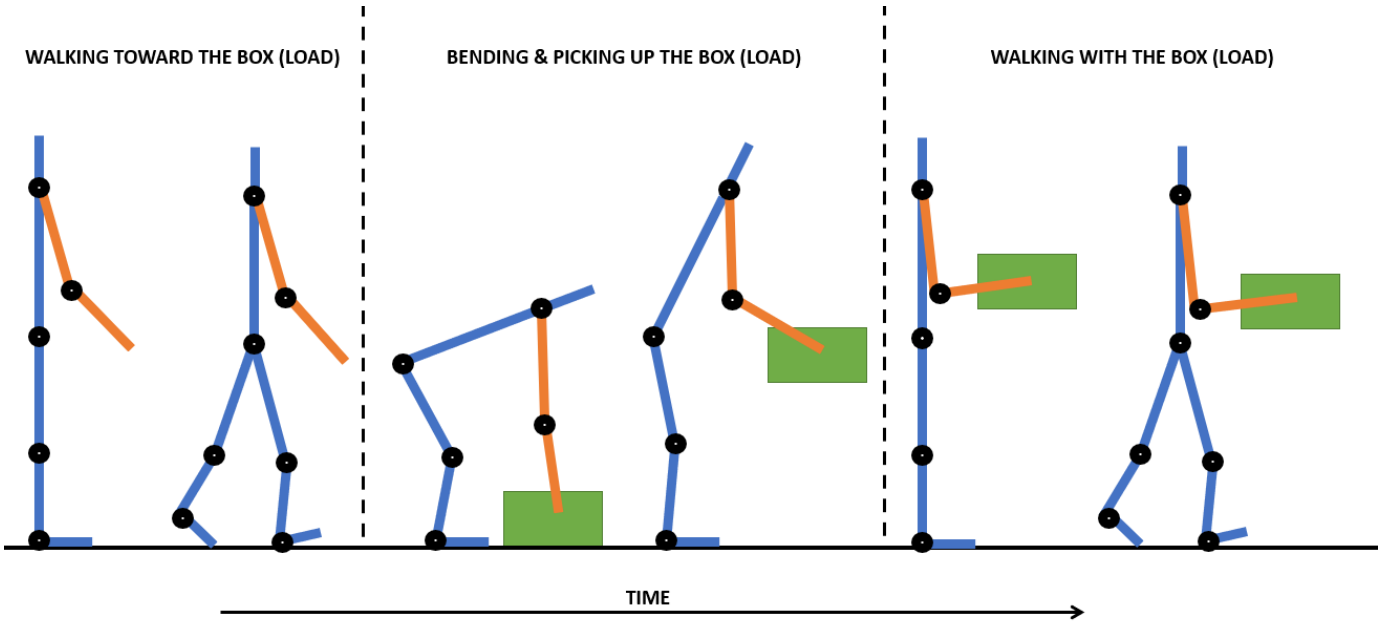

Fig. 3 : EXPERIMENTAL GAIT TASK REPRESENTATION

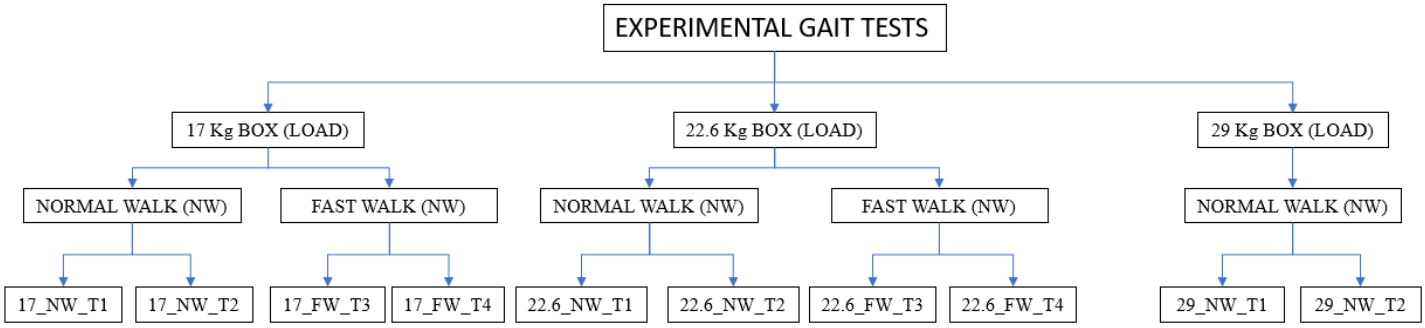

Fig. 4 : FLOW CHART OF TESTS CONDUCTED DURING EXPERIMENTAL GAIT TASK

TABLE 4 gives information about the nomenclature used for the GAIT experiments conducted for the given experimental task. The task has been segmented into various phases as represented in Fig. 3 in order to simplify and easily understand the mechanics that is being followed.

TABLE 4 : NOMENCLATURE FOR EXPERIMENTAL GAIT TEST

S.No.	TEST-NOMENCLATURE	DESCRIPTION
1	17_NW_T1	Normal pace walk with test load of 17 Kg – trial 1(trial 1 for normal walk case)
2	17_NW_T2	Normal pace walk with test load of 17 Kg – trial 2(trial 1 for fast normal case)
3	17_FW_T3	Fast pace walk with test load of 17 Kg – trial 3 (trial 1 for fast walk case)
4	17_FW_T4	Fast pace walk with test load of 17 Kg – trial 4 (trial 2 for fast walk case)
5	22.6_NW_T1	Normal pace walk with test load of 22.6 Kg – trial 1(trial 1 for normal walk case)
6	22.6_NW_T2	Normal pace walk with test load of 22.6 Kg – trial 2(trial 1 for fast normal case)
7	22.6_FW_T3	Fast pace walk with test load of 22.6 Kg – trial 3 (trial 1 for fast walk case)
8	22.6_FW_T4	Fast pace walk with test load of 22.6 Kg – trial 4 (trial 2 for fast walk case)
9	29_NW_T1	Normal pace walk with test load of 29 Kg – trial 1(trial 1 for normal walk case)
10	29_NW_T3	Normal pace walk with test load of 29 Kg – trial 2(trial 1 for fast normal case)

B. JOINT ROM, VELOCITY, ACCLERATION AND MOMENT

The experimental information about joint ROM, velocity and acceleration is useful in selection of actuators and batteries for the robot exoskeleton.

The joint ROM gives information about the extreme ends of the human joints for a given task. This is helpful in determining if a certain DOF requires actuation which otherwise may have been deemed less important.

The joint velocity, acceleration and moment is useful in determining the exoskeletons actuator specification such as the motor's maximum toque, etc. The gear ratio for the gear drive can also be determined using this information to get the desired maximum output torque. Knowing the average torque requirement and average joint velocity, the battery size can be estimated for a given expected time of usage.

The maximum values for of data for all tests are compiled for one soldier in the following table to understand and find general trend that is being followed. The absolute maximum for all test is compiled at the end of this section which is used later in this chapter to find desired motor specifications.

There are slight discrepancies in the test maximum observed which are due to unexpected and dynamic nature of walking (i.e. a person while walking may encounter uneven surface or a higher than usual impact of the foot on the ground, etc.). If these discrepancies are overlooked, they tend to follow a general pattern.

TABLE 3 gives information regarding the joint ROM in the sagittal plane as it is the plane that we are concerned with for the purpose of this study as the maximum movement happens about this plane.

It is observed from TABLE 5 that the joint ROM for a joint stay almost about the same regardless if the subject is walking fast or slow. There is a slight increase in ROM for elbow as the weight is increased (this much change is negligible). It can be explained as the moment arm about the weight is maximum and the bicep muscles which are carrying the load are small and relatively weak group of muscles thus the ROM is more.

TABLE 5 : JOINT RANGE OF MOTION (ROM) IN SAGITTAL PLANE – EXPERIMENTAL GAIT TASK

UNIT : Degrees		**NW_T1**	**NW_T2**	**FW_T3**	**FW_T4**
17 Kg	**SHOULDER**	-3.09 to 78.74	-7.391 to 78.67	-7.91 to 80.128	-8.59 to 80.78
	ELBOW	1.38 to 96.25	1.43 to 102.1	-0.23 to 110.58	-0.68 to 111.73
	LUMBAR	-47.61 to 4.58	-47.96 to 2.86	-44.69 to 7.85	-41.82 to 10.31
22.6 Kg	**SHOULDER**	-13.21 to 76.54	-11.23 to 78.49	-19.86 to 77.92	-15.47 to 79.83
	ELBOW	1.11 to 114.25	0.11 to 123.64	-2.60 to 127.71	-0.05 to 119.86

	LUMBAR	-46.41 to 6.53	-47.55 to 5.15	-42.24 to 2.93	-44.25 to 4.99
29 Kg	**SHOULDER**	-25.78 to 76.20	-27.50 to 85.94		
	ELBOW	-0.65 to 123.76	0.74 to 119.46		
	LUMBAR	-42.27 to 6.02	-43.83 to 3.23		

The joint velocities in TABLE 6 are higher for fast walk cases which is as expected; however, the maximum velocity more or less is about the same for different box load that is to be carried. It can be explained by need for lower body joint to travel at a higher joint velocity to increase the pace at which the body moves forward. The information about joint velocity is useful in selection of gear ratio and actuator as it gives the joint velocity that the actuator should be capable of supporting.

TABLE 6 : MAXIMUM JOINT VELOCITY IN SAGITTAL PLANE –ALL EXPERIMENTAL GAIT TASK

UNIT : Degrees/s		**NW_T1**	**NW_T2**	**FW_T3**	**FW_T4**
17 Kg	**SHOULDER**	157.79	175.90	217.72	197.67
	ELBOW	219.44	193.32	222.88	277.31
	LUMBAR	92.67	100.61	103.71	86.52
22.6 Kg	**SHOULDER**	178.82	219.90	258.06	227.22
	ELBOW	250.44	266.43	319.71	226.32
	LUMBAR	100.15	96.82	96.83	92.07
29 Kg	**SHOULDER**	203.97	198.24		
	ELBOW	219.44	220.02		
	LUMBAR	96.83	95.11		

The joint acceleration in TABLE 7 are higher for fast walk cases particularly for lower body joints and lumbar joint. This is due to the nature of the task assigned, in which the shoulder and elbow angles stay nearly the same with little movement. The same result is observed for different weight of the box carried.

TABLE 7 : MAXIMUM JOINT ACCLERATION IN SAGITTAL PLANE – ALL EXPERIMENTAL GAIT TASK

UNIT : Degrees/s^2		**NW_T1**	**NW_T2**	**FW_T3**	**FW_T4**
17 Kg	**SHOULDER**	1840.91	1428.4	2589.2	1497.7
	ELBOW	2704.53	2579.5	1663.9	1787.1
	LUMBAR	499.62	497.84	740.83	531.13
22.6 Kg	**SHOULDER**	1303.77	-2360	2997.66	2677.43
	ELBOW	2598.36	2516.4	4839.77	1994.46

	LUMBAR	647.1	559.78	856.57	791.46
29 Kg	**SHOULDER**	1367.42	3606.77		
	ELBOW	2715.87	2361.73		
	LUMBAR	794.12	643.43		

The joint reaction moment in TABLE 8 is useful in finding the actuator torque required and sets the minimum limit for joint torque needed. This information is important in selection of right actuator for the exoskeleton which is expected to perform the given task. It is observed from TABLE 8 that the joint torque stays about the same for both fast and normal walk however substantially increase as the load being carried is increased which is expected since moment is directly proportional to the load carried.

TABLE 8 : MAXIMUM JOINT MOMENT IN SAGITTAL PLANE – ALL EXPERIMENTAL GAIT TASK

UNIT : N-m		**NW_T1**	**NW_T2**	**FW_T3**	**FW_T4**
17 Kg	**SHOULDER**	26.34	27.90	28.68	27.46
	ELBOW	27.86	27.59	27.69	27.78
	LUMBAR	80.20	84.27	82.89	76.47
22.6 Kg	**SHOULDER**	36.04	35.71	34.36	34.09
	ELBOW	34.76	35.41	34.05	35.42
	LUMBAR	80.77	95.49	136.76	132.23
29 Kg	**SHOULDER**	32.36	37.94		
	ELBOW	32.83	32.2		
	LUMBAR	149.28	185.81		

The information from TABLE 5 to TABLE 8 were to get an understanding of how the parameters behave with changing conditions and get a general trend which can be used to extrapolate the result and be used in determining the factor of safety while selecting the actuator.

TABLE 9 complies the absolute maximum values observed across all tests and weights which is actually used to calculate the minimum required motor parameter.

TABLE 9 : MAXIMUM JOINT MOMENT IN SAGITTAL PLANE – AMONG ALL EXPERIMENTAL GAIT TASK

	VELOCITY (Degrees/s)	**ACCLERATION (Degrees/s^2)**	**MOMENT (N-m)**
SHOULDER	258.06	3606.77	37.94
ELBOW	319.71	4839.77	35.42
LUMBAR	103.71	856.57	185.81

The information from TABLE 9 is used in the next section of this chapter to calculate the required motor torque, gear ratio, recommended factor of safety, etc.

2.4 ACTUATOR SELECTION

Actuators is a component that is responsible for the movement of the machine or mechanism. It is very important to select the right type and specification of the actuator as it directly affects the weight, performance, efficiency and the power consumption.

Selection of actuator is of high importance particularly for applications in exoskeleton where the space available is limited and the performance characteristic are high.

A. TYPES OF ACTUATOR

The actuators are classified based on the type of motion they exhibit and the power supply used. This is important as the constraint of the robot design or any other criterial may require a particular type of actuator over other thus understanding the advantages and disadvantages of each type of actuator is important in selection of the actuator.

❖ **BASED ON MOTION**

- **LINEAR**

  It creates motion in a straight line when a power source is supplied to it. They are primarily used in machine tools, valves, dampers, etc.

  Examples – Screw, CAM, piston type hydraulic and pneumatic actuators, etc.

- **ROTARY**

  It creates rotary motion when a power source is supplied to it. These are one of the most commonly used actuators with application ranging from electric vehicles to vacuum cleaners.

  Examples – Stepper motors, DC motors, Rotary hydraulic and pneumatic actuators (turbine type)

❖ **BASED ON POWER SUPPLY**

- **ELECTRIC**

  Electric actuators use electricity as the source of power to generate movement, usually rotary. The current supply can be either AC or DC, however for majority of application a DC motors are used.

- **HYDRAULIC**

  It uses hydraulic fluid under pressures to produce movement and work as an actuator. It uses fluid power as to cause actuation movement. It can produce very high output force.

- **PNEUMATIC**

  It is similar to hydraulic actuators except it uses compressed air instead of hydraulic fluid. It is not able to generate as much force as hydraulic actuator due to compressible nature of gases (primarily air)

- **PIEZOELECTRIC**

  They produce small displacement and high force when a voltage is applied across them

B. MOTOR SELECTION CRITERIA FOR EXOSKELETON

The criteria for selection of actuator for use in exoskeleton is very specific. There are a lot of exoskeletons that use electric, hydraulic, pneumatic actuators. There are exoskeleton designs that require linear actuators as opposed to rotary ones which tend to be more common.

The type of actuator selected depends on a lot of factors such as the usage, conditions of usage, load capacity, applications, etc.

The selection criteria for the exoskeleton in this study is as follows-

- ❖ High power to weight ratio
- ❖ Compact in size
- ❖ There overall weight should be as less as possible
- ❖ The motor should have high acceleration (i.e., good responsiveness)
- ❖ It should not be harmful and/or toxic if a fluid is used (as is the case with hydraulic actuators)
- ❖ There should not be leakages if a fluid is used

Rotary actuators are easy to incorporate into the exoskeleton design and will also be lighter in weight since less material is required to make complex mechanism.

Electric motor does not require a compressor which reduces the overall weight of the exoskeleton and as compared to pneumatic and hydraulic actuators. Electric motors also provide just as high torque as pneumatic actuators. Hydraulic actuators provide higher force outputs than electric and pneumatic actuators but require fluids which can leak (common problem in hydraulics).

Brushless DC (BLDC) motor is chosen for application in the current study due to its advantages and the exoskeleton requirements. Since the exoskeleton is powered by a battery thus a DC motor is used.

Brushless DC motor is chosen instead of brushed DC motor as they have longer life (due to no contact between moving part i.e., no brush), high efficiency and high power to weight ratio.

C. DETERMINING MOTOR SPECIFICATIONS

The motor specifications are selected based on experimental data. The information regarding joint speed and torque is used. One of the parameters has to be assumed initially either input speed or input torque to find the motor's minimum requirements.

The formula used for calculations are –

$$GR = \frac{\tau_0}{\tau_i} = \frac{N_i}{N_0} \quad (1)$$

$$P = \frac{2\pi\tau_i N_i}{60} = \frac{2\pi\tau_0 N_0}{60} \quad (2)$$

Where,

TABLE 10 : SYMBOL DESCRIPTION FOR eqn.(1) and eqn.(2)

S.No.	PARAMETER	DESCRIPTION	UNITS
1	GR	Gear Ratio	-
2	τ_i	Motor's input torque	Nm
3	τ_0	Output torque	Nm
4	N_i	Motor's input speed	RPM
5	N_0	Output speed	RPM
6	P	Power	W

The actuator specifications for elbow & lumbar/waist joint are found using information from TABLE 9 with the assumption that maximum torque at the joint occurs at the maximum speed of the joint. This assumption is taken in order to account for the worst-case scenario and to ensure that the motor works effectively.

Also, $(\tau_0 N_0)_{max} \leq (\tau_0)_{max}(N_0)_{max}$ thus the assumption is valid.

The factor of safety (FOS) usually is taken as 1.5, for current study this value of FOS is used.

❖ ELBOW JOINT

From TABLE 9 maximum elbow joint torque and speed are found to be as, $\tau_0 = 35.42\ Nm$ and $N_0 = \frac{319.71}{60} = 5.318\ RPM$

Therefore, $\tau_i N_i = \tau_0 N_0 = (35.42)(5.318) = 188.375$

Assuming motors input speed from 1000 to 10000 RPM with an increment of 1000 RPM(except for 1 case where increment is of 500 RPM).

The input speed, input torque and gear ratio for elbow joint are tabulated in TABLE 11 and is used to finalize a motor that closely matches them and is commercially available.

TABLE 11 : MOTOR'S SPEED TORQUE AND GEAR RATIO REQUIRMENT FOR ELBOW EXOSKELETON

S.No.	MOTOR'S INPUT SPEED (RPM)	MOTOR'S INPUT TORQUE (N-m)	GEAR RATIO
1	500	0.37675	94.0146
2	1000	0.188375	188.0292
3	2000	0.0941875	376.0584
4	3000	0.0627916	564.0882
5	4000	0.04709375	752.1168
6	5000	0.037675	940.146
7	6000	0.03139583	1128.175
8	7000	0.026910713	1316.204
9	8000	0.023546875	1504.234
10	9000	0.02093055	1692.263
11	10000	0.0188375	1880.292

- **LUMBAR/WAIST JOINT**

From TABLE 9 maximum lumbar/waist joint torque and speed are found to be as, $\tau_0 = 35.42\ Nm$ and $N_0 = \frac{103.71}{60} = 1.7285\ RPM$

Therefore, $\tau_i N_i = \tau_0 N_0 = (185.81)(1.7285) = 321.172585$

Assuming motors input speed from 1000 to 10000 RPM with an increment of 1000 RPM (except for 1 case where increment is of 500 RPM).

TABLE 12 : MOTOR'S SPEED TORQUE AND GEAR RATIO REQUIRMENT FOR LUMBAR/WAIST EXOSKELETON

S.No.	MOTOR'S INPUT SPEED (RPM)	MOTOR'S INPUT TORQUE (N-m)	GEAR RATIO
1	500	0.64234517	289.26815
2	1000	0.321172585	578.5363
3	2000	0.160586	1157.075

4	3000	0.107057	1735.617
5	4000	0.08029	2314.236
6	5000	0.064234517	2892.682
7	6000	0.05352876	3471.218
8	7000	0.04588179	4049.755
9	8000	0.0401465	4628.299
10	9000	0.03568584278	5206.827
11	10000	0.0321172585	5785.363

The input speed, input torque and gear ratio for lumbar/waist joint are tabulated in TABLE 12 and is used to finalize a motor that closely matches them and is commercially available.

D. MOTOR SELECTION

The motor torque, motor speed and gear ratio tabulated in TABLE 9 and TABLE 10 is used select a commercially available motor. It is preferred to select a motor that consumes less power as higher power consumption causes the battery to be lager for the same time of operation. Batteries are the heaviest component in an exoskeleton thus it is preferred to keep them as light and compact as possible.

Power of motor required for elbow and lumbar/waist joint can be found using the maximum torque and maximum speed of the joint from TABLE 7. The power value from this will be more than the actual maximum power from the experiment conducted as shown by eqn. () but is still taken so as to account for the worst-case scenario and choose the most optimum motor.

$$P_{elbow} = \frac{2\pi(35.42)(5.318)}{60} = 19.725\ W$$

$$P_{lumbar/waist} = \frac{2\pi(185.81)(1.7285)}{60} = 33.633\ W$$

The power of the elbow joint is multiplied with a FOS of 1.5 to ensure that the motor selected is well within the requirements as the nature of the test itself is dynamic in nature and also dependant on the body weight of the wearer.

$$P'_{elbow} = 1.5(P_{elbow}) = 29.6\ W \approx 30\ W$$

$$P'_{lumbar/waist} = 1.5(P_{lumbar/waist}) = 50.4495\ W \approx 50\ W$$

Since the torque required by the lumbar joint is substantially more as it also has to support the entire upper body, thus may require a larger motor than 50 W if the intended usage may require a load of more than 29 Kg.

The purpose of the exoskeleton being studied is for defence application thus strength augmentation is of primary concern thus it is recommended that a larger motor be used for lower back as while picking up any object the lumbar muscles are the prime movers.

2 motors selected that fulfil the criteria for exoskeleton are-

- **MAXON EC90 Flat, 90 W**

  It is a 90 W motor that is capable of providing a maximum continuous torque of 0.533 Nm and a nominal speed of 2080 RPM. The speed of the motor in absence of load is 2080 RPM.

  From TABLE 7 we can see that the input speeds from 1000 to 2000 RPM are capable of satisfying the needs for both the elbow and lumbar/waist exoskeleton and are within the motor's capability.

  The gear ratio selected for elbow exoskeleton is 188.0292 which requires an input torque of 0.188375 Nm which the motor is more than capable of providing. Since 188.0292 gear ratio is difficult to get commercially thus a more readily available ratio of 200 is chosen that puts the input torque requirement at 0.1771. Considering the maximum torque capability (0.533 Nm) of the motor the weight that can be expected to be lifted (held at the location) by the exoskeleton is about 31 Kg (assuming it is providing all the assistance), taking the length of the moment arm about elbow as 29.856 cm from TABLE 2.

  If this motor is selected for lumbar/waist exoskeleton then a gear ratio of 578.5363 is selected which requires an input torque of about 0.31172585 Nm. The gear ratio more readily available commercially will be 580 or 600 which will require an input torque of about 0.32036 Nm and 0.309683Nm which is also well within the motor's capability. The maximum load that the motor will be able to assist with is about 66 Kg, taking the length of the moment arm about the lumbar joint from TABLE 2

  The motor for the lumbar spine can be of a higher capacity since the weight of the trunk itself significantly large thus there will be a compromise between the speed and maximum load that can be lifted. This motor however is still more than sufficient to assist while walking as then the moment arm of the lumbar joint is small and requires less assistance thus less torque. The maximum assistance needed is while lifting and if a compromise is made with how fast the load is lifted (speed) at loads heavier than the experimental data of 29 Kg (assuming it is providing all the assistance which won't actually be the case) then for that case this motor works perfectly.

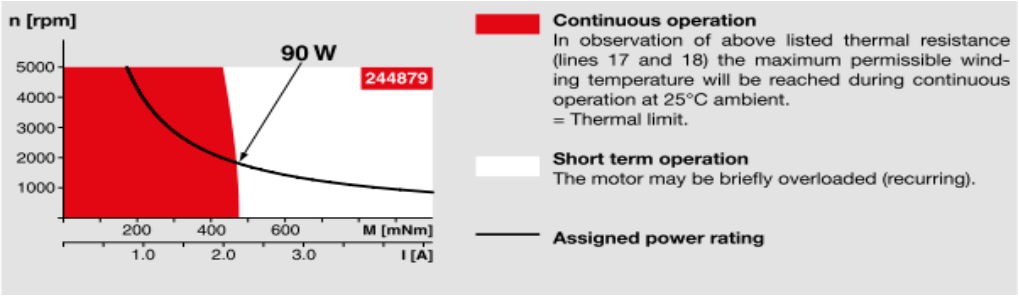

Fig. 5 : MAXON EC90 FLAT, 90W MOTOR – SPEED VS TORQUE & SPEED VS CURRENT GRAPH (ByMAXON MOTORS; https://www.maxongroup.com/medias/sys_master/root/8825435389982/17-EN-271.pdf)

TABLE 13 : MOTOR SPECIFICATION – MAXON EC90 FLAT, 90W MOTOR

S.No.	PARAMETER	UNITS	DATA/DESCRIPTION
1	Hall Sensor	-	Detects the presence/magnitude of the magnetic field whose strength is proportional to the output voltage It is used as position sensor (for permanent magnets)
2	No Load Speed	RPM	2080
3	Nominal Speed	RPM	1610
4	No Load Current	mA	135
5	Nominal Voltage	V	48
6	Max. Continuous Torque	mN-m	533
7	Stall Torque	mN-m	4570
8	Max. Continuous Current	A	2.27
9	Stall Current	A	21.1
10	Max. Efficiency	%	85
11	Terminal Resistance phase to phase	Ω	2.28
12	Terminal Inductance phase to phase	mH	2.5
13	Torque Constant	mN-m/A	217
14	Speed Constant	RPM/V	44
15	Mechanical Time Constant	ms	14.8
16	Rotor Inertia	$g\text{-}cm^2$	3060
17	Thermal Resistance of Housing - Ambient	K/W	1.91
18	Thermal Resistance of Winding - Housing	K/W	2.6
19	Thermal Time Constant Winding	s	46
20	Thermal Time Constant Motor	s	283
21	Ambient Temperature (Operating Temperature Range)	℃	-40℃ to 100℃
22	Max. Winding Temperature	℃	125℃
23	Axial Play (load <15N)	mm	0
24	Axial Play (load >15N)	mm	0.14
25	Max. Axial Load	N	12
26	Max. Radial Load (5mm from flange)	N	183
27	Number of Pole Pairs	-	12
28	Number of Phases	-	3
29	Weight of Motor	g	600

- **MAXON EC90 Flat, 260 W**

  It is a 260 W motor that is capable of providing a maximum continuous torque of 0.988 Nm and a nominal speed of 1780 RPM. The speed of the motor in absence of load is 2080 RPM.

From TABLE 7 we can see that the input speeds less than 2000 RPM are capable of satisfying the needs for both the elbow and lumbar/waist exoskeleton and are within the motor's capability.

This motor is only to be considered for lumbar exoskeleton as it draws a lot of power and provides very high values of torque which is not needed for elbow exoskeleton.

If the gear ratio selected for the lumbar/waist exoskeleton is 289.26815 which requires a motor input torque of about 0.6423 Nm at 500 RPM which is well within the motor's capability. The gear ratio 289.26815 will not be commercial thus is taken as 290 which is easier to find commercially, thus the input motor toque needed for a gear ratio of 290 is 0.6439. The maximum assistance that it can provide with this gear ratio is about 95.97 Kg (taking the length of the moment arm about elbow as 29.856 cm from TABLE).

If a higher gear ratio is feasible and the lumbar/waist exoskeleton's purpose is to maximize the strength augmentation then a gear ratio of 580 or 600 is able to augment the user's strength by up to 193.8 Kg and 200.5 Kg respectively (taking the length of the moment arm about elbow as 29.856 cm from TABLE 2)

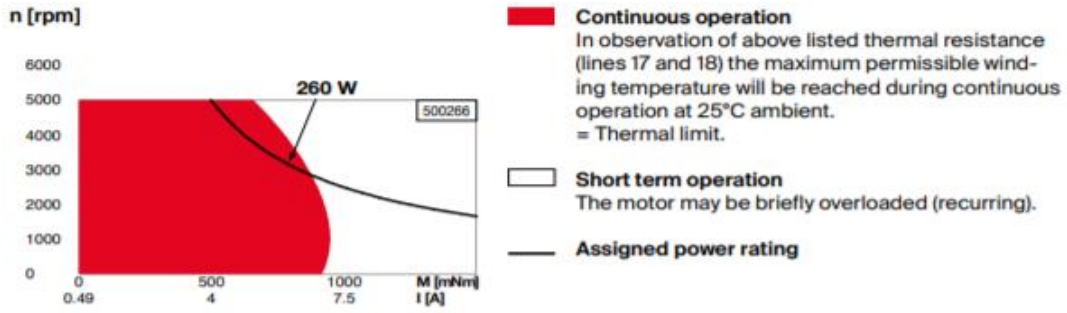

Fig. 6 : MAXON EC90 FLAT, 260W MOTOR – SPEED VS TORQUE & SPEED VS CURRENT GRAPH
(By MAXON MOTORS; https://www.maxongroup.com/medias/sys_master/root/8841186050078/EN-300.pdf)

TABLE 14 : MOTOR SPECIFICATION – MAXON EC90 FLAT, 260W MOTOR

S.No.	PARAMETER	UNITS	DATA/DESCRIPTION
1	Hall Sensor	-	Detects the presence/magnitude of the magnetic field whose strength is proportional to the output voltage It is used as position sensor (for permanent magnets)
2	No Load Speed	RPM	2080
3	Nominal Speed	RPM	1780
4	No Load Current	mA	490
5	Nominal Voltage	V	1780
6	Max. Continuous Torque	mN-m	988
7	Stall Torque	mN-m	14600
8	Max. Continuous Current	A	7.06

9	Stall Current	A	107
10	Max. Efficiency	%	87
11	Terminal Resistance phase to phase	Ω	0.28
12	Terminal Inductance phase to phase	mH	0.369
13	Torque Constant	mN-m/A	136
14	Speed Constant	RPM/V	70.2
15	Mechanical Time Constant	ms	7.66
16	Rotor Inertia	$g\text{-}cm^2$	5060
17	Thermal Resistance of Housing - Ambient	K/W	1.74
18	Thermal Resistance of Winding - Housing	K/W	1.82
19	Thermal Time Constant Winding	s	57
20	Thermal Time Constant Motor	s	258
21	Ambient Temperature (Operating Temperature Range)	℃	-40℃ to 100℃
22	Max. Winding Temperature	℃	125
23	Axial Play	mm	0.14
25	Max. Axial Load	N	34
26	Max. Radial Load (10mm from flange)	N	130
27	Number of Pole Pairs	-	11
28	Number of Phases	-	3
29	Weight of Motor	g	980

❖ FINALIZING MOTOR

- From the current study's perspective, the load lifted by the wearers is sub-maximal and also since the back muscles are among the strongest in the body thus MAXON EC90 Flat, 90 W motor is recommended and used for further study for both lumbar and elbow exoskeleton. The selected gear ratio for this motor is 200 for elbow exoskeleton and 580 for lumbar/waist exoskeleton.
- MAXON EC90 Flat, 260 W motor is recommended only if very large loads have to be lifted by the wearer as the power consumption is nearly 3 times the other MAXON EC90 Flat, 90 W motor.
- The MAXON EC90 Flat, 260 W is able to provide very large assistance only if the gear ratio is large (i.e., 580 or 600)

CHAPTER 3

3.1 INTRODUCTION

This chapter discusses the dynamics and kinematic equations of the body and robot exoskeleton. They kinematic and dynamic equations are of importance as they give us information about the work volume of the robot, joint singularities (inverse of jacobian is not defined) and the equation of motion equations that describes the motion of the system in terms of parameters such as angles, angular velocities, angular acceleration and torques.

In the exoskeleton the position and the speed of the joints of exoskeleton can be directly measured using sensors, which is fed into the controller.

The mathematical modelling of a complex system is hard and usually simplified with certain assumptions. This dynamics equation is useful in simulating and testing the working effectiveness of the robot.

The chapter derives and describes the dynamic model of the human body, robot and motor which is used in later chapter to for simulation and designing of the controller for the exoskeleton.

3.2 BODY KINEMATICS & DYNAMICS

NOTE : The dynamics and kinematic equations in this section are aimed at predicting joint reference torque, however this equation can also be used to represent full-body exoskeleton dynamics changing the values of mass, length and inertia from that of the human body to that of the exoskeleton links

The human body is simplified as 5 DOF and 2/3 DOF problem in the sagittal plane. When both the feet are on the ground (stance phase) the body follows 5 DOF dynamics, however during walking the body follows 5 DOF dynamics about the leg that is on the ground while the leg that is swinging follows a 2/3 DOF dynamics depending how it is modelled.

During walking phase, the zero-moment point (moment acting on the about this point is zero) is taken as the centre of the sole of foot while in the stance phase it is in between the two legs (i.e., doesn't lie on the body). It is important for maintaining balance, however is primarily of concern for lower body exoskeleton. Since the current study is on upper body exoskeleton and not on lower body exoskeleton thus an there is no need to study the kinematics and dynamics of the leg in the swing phase.

TABLE 15 comprises of all the parameters and symbols used that are used within this section (3.2) in order to derive the kinematic and dynamic equation of the human body assuming it as a 5 DOF planar joints.

Limitations of the assumption of the body as a 5 DOF kinematics is that since it does not account for movement in the coronal and transverse plane thus any movement will cause an error. The error will be small for small movements and can be neglected however for lar movements particularly in the coronal plane (abduction/adduction) will cause significant error.

The error for lumbar/waist joint is less due to the location and movement constraint of the joint thus this assumption will work well, however for elbow joint the movement about coronal plane will cause significantly large error thus while using this model to predict the joint torque should stop if the deflection in that plane is more than a pre-defined value.

This model is a good approximation to generate required joint torque for application specified which has movement primarily in the sagittal plane for picking and moving the objects. The aim is to not augment strength but to increase repetition at a given load by the wearer.

TABLE 15 : PARAMETERS AND SYMBOLS USED IN SEC. 3.2 (eqn. (5) to eqn. (79))

S.No.	PARAMETER	UNITS	DESCRIPTION
1	θ_1	Degree ($^\circ$)	Angle of rotation of Link 1 wrt. to horizontal
2	$\dot{\theta_1}$	rad./s	Angular Velocity of Link 1
3	$\ddot{\theta_1}$	Rad./s^2	Angular Acceleration of Link 1
4	θ_2	Degree ($^\circ$)	Angle of rotation of Link 2 wrt. to horizontal
5	$\dot{\theta_2}$	rad./s	Angular Velocity of Link 2
6	$\ddot{\theta_2}$	Rad./s^2	Angular Acceleration of Link 2
7	θ_3	Degree ($^\circ$)	Angle of rotation of Link 3 wrt. to horizontal
8	$\dot{\theta_3}$	rad./s	Angular Velocity of Link 3
9	$\ddot{\theta_3}$	rad./s^2	Angular Acceleration of Link 3
10	θ_4	Degree ($^\circ$)	Angle of rotation of Link 4 wrt. to horizontal
11	$\dot{\theta_4}$	rad./s	Angular Velocity of Link 4
12	$\ddot{\theta_4}$	rad./s^2	Angular Acceleration of Link 4

13	θ_5	Degree ($^\circ$)	Angle of rotation of Link 5 wrt. to horizontal
14	$\dot{\theta_5}$	rad./s	Angular Velocity of Link 5
15	$\ddot{\theta_5}$	rad./s^2	Angular Acceleration of Link 5
16	λ_2	Degree ($^\circ$)	$\theta_2 - \theta_1$
17	λ_3	Degree ($^\circ$)	$\theta_2 - \theta_3$
18	λ_4	Degree ($^\circ$)	$180 - \theta_4 - \theta_3$
19	λ_5	Degree ($^\circ$)	$\theta_4 - \theta_5$
20	X_1	m	X axis co-ordinate of tip of Link 1
21	Y_1	m	Y axis co-ordinate of tip of Link 1
22	X_2	m	X axis co-ordinate of tip of Link 2
23	Y_2	m	Y axis co-ordinate of tip of Link 2
24	X_3	m	X axis co-ordinate of tip of Link 3
25	Y_3	m	Y axis co-ordinate of tip of Link 3
26	X_4	m	X axis co-ordinate of tip of Link 4
27	Y_4	m	Y axis co-ordinate of tip of Link 4
28	X_5	m	X axis co-ordinate of tip of Link 5
29	Y_5	m	Y axis co-ordinate of tip of Link 5
30	L_1	m	Length of Link 1 (Shank)
31	L_2	m	Length of Link 2 (thigh)
32	L_3	m	Length of Link 3 (torso)

33	L_4	m	Length of Link 4 (shoulder)
34	L_5	m	Length of Link 5 (elbow + hand/2 : as it is assumed that the load is carried at the mid-point of hand)
35	L_{1c}	m	Length of centroid of Link 1 from origin (i.e., base of Link 1)
36	L_{2c}	m	Length of centroid of Link 2 from base of Link 2 (joint 2)
37	L_{3c}	m	Length of centroid of Link 3 from base of Link 3 (joint 3)
38	L_{4c}	m	Length of centroid of Link 4 from base of Link 4 (joint 4)
39	L_{5c}	m	Length of centroid of Link 5 from base of Link 5 (joint 5)
40	M_1	Kg	Mass of Shank (link 1)
41	M_2	Kg	Mass of thigh (link 2)
42	M_3	Kg	Mass of torso and head (link 3)
43	M_4	Kg	Mass of shoulder (link 4)
44	M_5	Kg	Mass of elbow and hand (link 5)
45	M_{15}	Kg	$M_1 + M_2 + M_3 + M_4 + M_5$
46	M_{25}	Kg	$M_2 + M_3 + M_4 + M_5$
47	M_{35}	Kg	$M_3 + M_4 + M_5$
48	M_{45}	Kg	$M_4 + M_5$
49	L	-	Lagrangian

50	T	Kg-m^2/s	Total Kinetic Energy
51	U	Kg-m^2/s	Total Potential Energy
52	τ_1	N-m	Toque at joint 1
53	τ_2	N-m	Toque at joint 2
54	τ_3	N-m	Toque at joint 3
55	τ_4	N-m	Toque at joint 4
56	τ_5	N-m	Toque at joint 5
57	I_1	Kg-m^2	Moment of Inertia about centroid for shank and foot
58	I_2	Kg-m^2	Moment of Inertia about centroid for thigh
59	I_3	Kg-m^2	Moment of Inertia about centroid for torso and head
60	I_4	Kg-m^2	Moment of Inertia about centroid for shoulder
61	I_5	Kg-m^2	Moment of Inertia about centroid for elbow and hand
62	I_{15}	Kg-m^2	$I_1 + I_2 + I_3 + I_4 + I_5$
63	I_{25}	Kg-m^2	$I_2 + I_3 + I_4 + I_5$
64	I_{35}	Kg-m^2	$I_3 + I_4 + I_5$
65	I_{45}	Kg-m^2	$I_4 + I_5$
66	C_1	-	$\cos(\theta_1)$
67	C_2	-	$\cos(\theta_2)$
68	C_3	-	$\cos(\theta_3)$
69	C_4	-	$\cos(\theta_4)$
70	C_5	-	$\cos(\theta_5)$
71	C_{12}	-	$\cos(\theta_1 - \theta_2)$
72	C_{13}	-	$\cos(\theta_1 - \theta_3)$
73	C_{14}	-	$\cos(\theta_1 - \theta_4)$
74	C_{15}	-	$\cos(\theta_1 - \theta_5)$
75	C_{23}	-	$\cos(\theta_2 - \theta_3)$
76	C_{24}	-	$\cos(\theta_2 - \theta_4)$

77	C_{25}	-	$\cos(\theta_5 - \theta_5)$
78	C_{34}	-	$\cos(\theta_3 - \theta_4)$
79	C_{35}	-	$\cos(\theta_3 - \theta_5)$
80	C_{45}	-	$\cos(\theta_4 - \theta_5)$
81	S_{12}	-	$\sin(\theta_1 - \theta_2)$
82	S_{13}	-	$\sin(\theta_1 - \theta_3)$
83	S_{14}	-	$\sin(\theta_1 - \theta_4)$
84	S_{15}	-	$\sin(\theta_1 - \theta_5)$
85	S_{23}	-	$\sin(\theta_2 - \theta_3)$
86	S_{24}	-	$\sin(\theta_2 - \theta_4)$
87	S_{25}	-	$\sin(\theta_5 - \theta_5)$
88	S_{34}	-	$\sin(\theta_3 - \theta_4)$
89	S_{35}	-	$\sin(\theta_3 - \theta_5)$
90	S_{45}	-	$\sin(\theta_4 - \theta_5)$

5 DOF REPRESENTATION

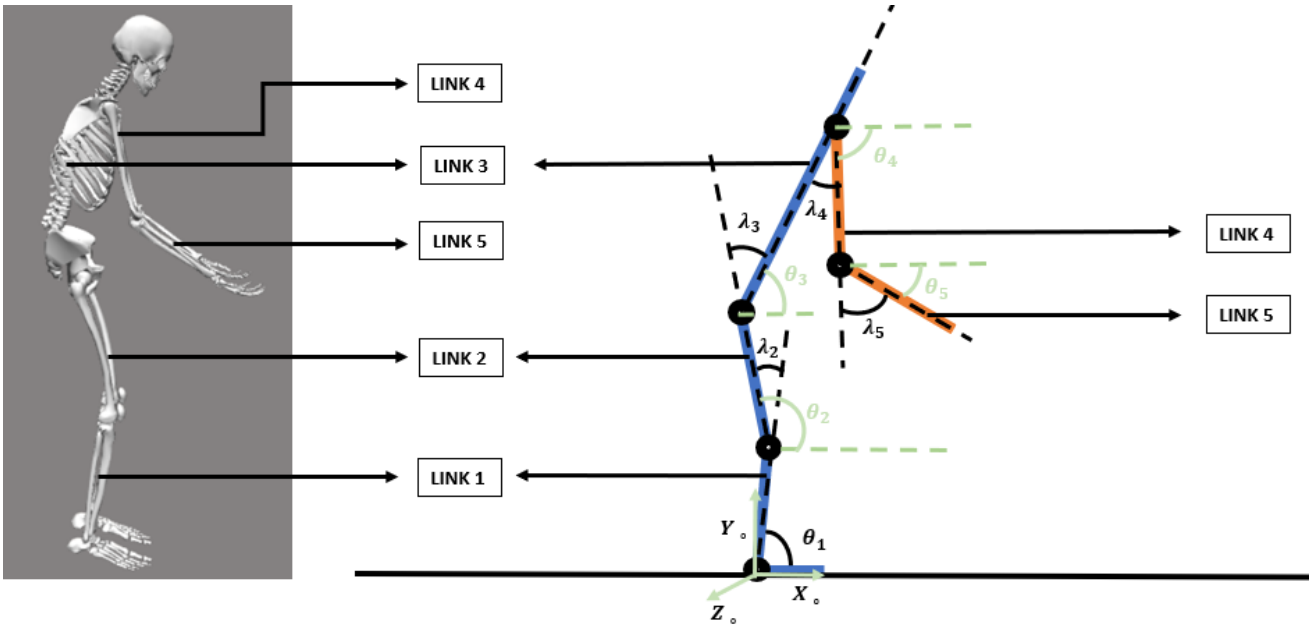

Fig. 7 : SIMPLIFIED REPRESENTATION OF HUMAN BODY/FULL BODY EXOSKELETON (5 DOF)

The dynamics represented by 5 DOF planar links for motion in sagittal plane assumes that since the height and mass of the foot is not substantial enough to cause any significant impact thus is neglected in link 1's mass and height and is thus only the mass and length of the shank. The lower arm joint (link 5) length is the length of forearm plus half the length of hand as it is assumed that the person lifts objects through the centre of their hand. This assumption is valid

as it is the case often and also if not, the error is negligible since its mass, and length are very small considered to forearm.

The mass of link 3 is the summation of mass of torso and mass of the head. Similarly, the mass of link 5 is the summation of the mass of forearm and mass of the hand. The centre of mass for link 3 and link 5 is found using the formula for centre of mass,

$$COM = \frac{(MASS\ 1)(DISTANCE\ FROM\ REFERENCE)+\cdots(MASS\ n)(DISTANCE\ FROM\ REFERENCE)}{(MASS\ 1+\cdots MASS\ n)} \quad (3)$$

The reference for torso (link 3) is taken as the lumbar joint and for the lower arm (link 5) it is taken as the elbow joint.

The moment of inertia for the new shifted centre of mass is found using the formula,

$$I = I_1 + M_1 r_1^2 + \cdots I_n + M_n r_n^2 \quad (4)$$

$I_1 \ldots I_n$ are the moment of inertia about their centroid and $r_1 \ldots r_n$ is the distance of their respective centroid/COM to the centroid/COM of the total system which is found using the eqn. (3)

TABLE 16 gives information regarding mass, centre of mass and moment of inertia for the simplified representation of human body. This information is found using TABLE 2, TABLE 3, eqn. (3) and eqn. (4) in conjunction to the assumptions followed as previously mentioned. The data from TABLE 5 is used in this section and subsequent chapters if there is a mention of the human body dynamics or kinematics.

TABLE 16 : THE MASS, CENTRE OF MASS AND MOMENT OF INERTIA OF LINKS : SIMPLIFIED HUMAN BODY REPRESENTATION

	MASS (Kg)	**LENGTH (m)**	**LENGTH UPTO CENTRE OF MASS OF i^{th} LINK FROM i^{th} JOINT (m)**	**MOMENT OF INERTIA ABOUT CENTRE OF MASS (Kg-m^2)**
LINK 1	2.8145	0.37305	0.2067	0.002229480915
LINK 2	9.204	0.4932	0.2913	0.07797041217
LINK 3	32.76	0.5756	0.5035	3.365423009
LINK 4	1.7615	0.23213	0.1542	0.0005465727083
LINK 5	1.4495	0.3278945	0.1625	0.00329483

❖ KINEMATICS

TABLE 17 : DH PARAMETERS FOR 5 DOF PLANAR MODEL

	α	a	θ	d
1	0	0	θ_1	0
2	0	L_1	λ_2	0
3	0	L_2	360-λ_3	0
4	0	L_3	180+ λ_4	0
5	0	L_4	λ_5	0
6	0	L_5	0	0

Rotation of link 1 wrt. base frame as homogeneous transformation matrix is,

$$ {}^{0}_{1}T = \begin{bmatrix} \cos(\theta_1) & -\sin(\theta_1) & 0 & L_1\cos(\theta_1) \\ \sin(\theta_1) & \cos(\theta_1) & 0 & L_1\sin(\theta_1) \\ 0 & 0 & 1 & 0 \\ 0 & 0 & 0 & 1 \end{bmatrix} \quad (5) $$

Coordinate transformation of link 2 wrt. joint 2 as homogeneous transformation matrix is,

$$ {}^{1}_{2}T = \begin{bmatrix} \cos(\lambda_2) & -\sin(\lambda_2) & 0 & L_2\cos(\lambda_2) \\ \sin(\lambda_2) & \cos(\lambda_2) & 0 & L_2\sin(\lambda_2) \\ 0 & 0 & 1 & 0 \\ 0 & 0 & 0 & 1 \end{bmatrix} \quad (6) $$

Coordinate transformation of link 3 wrt. joint 3 as homogeneous transformation matrix is,

$$ {}^{2}_{3}T = \begin{bmatrix} \cos(\lambda_3) & \sin(\lambda_3) & 0 & L_3\cos(\lambda_3) \\ -\sin(\lambda_3) & \cos(\lambda_3) & 0 & -L_3\sin(\lambda_3) \\ 0 & 0 & 1 & 0 \\ 0 & 0 & 0 & 1 \end{bmatrix} \quad (7) $$

Coordinate transformation of link4 wrt. joint 4 as homogeneous transformation matrix is,

$$ {}^{3}_{4}T = \begin{bmatrix} -\cos(\lambda_4) & \sin(\lambda_4) & 0 & -L_4\cos(\lambda_4) \\ -\sin(\lambda_4) & -\cos(\lambda_4) & 0 & -L_4\sin(\lambda_4) \\ 0 & 0 & 1 & 0 \\ 0 & 0 & 0 & 1 \end{bmatrix} \quad (8) $$

Coordinate transformation of link 5 wrt. joint 5 as homogeneous transformation matrix is,

$$ {}^{4}_{5}T = \begin{bmatrix} \cos(\lambda_5) & -\sin(\lambda_5) & 0 & L_5\cos(\lambda_5) \\ \sin(\lambda_5) & \cos(\lambda_5) & 0 & L_5\sin(\lambda_5) \\ 0 & 0 & 1 & 0 \\ 0 & 0 & 0 & 1 \end{bmatrix} \tag{9} $$

Coordinate transformation of link 5 wrt. base frame (joint 1) as homogeneous transformation matrix is,

$$ {}^{0}_{5}T = {}^{0}_{1}T\,{}^{1}_{2}T\,{}^{2}_{3}T\,{}^{3}_{4}T\,{}^{4}_{5}T \tag{10} $$

$$ {}^{0}_{5}T = {}^{0}_{1}T\,{}^{1}_{2}T\,{}^{2}_{3}T\,{}^{3}_{4}T\,{}^{4}_{5}T = \begin{bmatrix} -\cos(\theta_1+\lambda_2+\lambda_3+\lambda_4+\lambda_5) & -\sin(\theta_1+\lambda_2+\lambda_3+\lambda_4+\lambda_5) & 0 & L_1\cos(\theta_1)+L_2\cos(\theta_1+\lambda_2)+L_3\cos(\theta_1+\lambda_2+\lambda_3)-L_4\cos(\theta_1+\lambda_2+\lambda_3+\lambda_4)-L_5\cos(\theta_1+\lambda_2+\lambda_3+\lambda_4+\lambda_5) \\ \sin(\theta_1+\lambda_2+\lambda_3+\lambda_4+\lambda_5) & -\cos(\theta_1+\lambda_2+\lambda_3+\lambda_4+\lambda_5) & 0 & L_1\sin(\theta_1)+L_2\sin(\theta_1+\lambda_2)+L_3\sin(\theta_1+\lambda_2+\lambda_3)+L_4\sin(\theta_1+\lambda_2+\lambda_3+\lambda_4)+L_5\sin(\theta_1+\lambda_2+\lambda_3+\lambda_4+\lambda_5) \\ 0 & 0 & 1 & 0 \\ 0 & 0 & 0 & 1 \end{bmatrix} \tag{11} $$

The co-ordinates of the end of link 5 is given as,

$$ \begin{bmatrix} X \\ Y \\ \phi \end{bmatrix} = \begin{bmatrix} L_1\cos(\theta_1)+L_2\cos(\theta_1+\lambda_2)+L_3\cos(\theta_1+\lambda_2+\lambda_3)-L_4\cos(\theta_1+\lambda_2+\lambda_3+\lambda_4)-L_5\cos(\theta_1+\lambda_2+\lambda_3+\lambda_4+\lambda_5) \\ L_1\sin(\theta_1)+L_2\sin(\theta_1+\lambda_2)+L_3\sin(\theta_1+\lambda_2+\lambda_3)+L_4\sin(\theta_1+\lambda_2+\lambda_3+\lambda_4)+L_5\sin(\theta_1+\lambda_2+\lambda_3+\lambda_4+\lambda_5) \\ \theta_1+\lambda_2+\lambda_3+\lambda_4+\lambda_5+440 \end{bmatrix} \tag{12} $$

Jacobian matrix is used to convert joint space into cartesian space and vice versa. The jacobian matrix is given as,

$$ J = \begin{bmatrix} \frac{\partial X}{\partial\theta_1} & \frac{\partial X}{\partial\lambda_2} & \frac{\partial X}{\partial\lambda_3} & \frac{\partial X}{\partial\lambda_4} & \frac{\partial X}{\partial\lambda_5} \\ \frac{\partial Y}{\partial\theta_1} & \frac{\partial Y}{\partial\lambda_2} & \frac{\partial Y}{\partial\lambda_3} & \frac{\partial Y}{\partial\lambda_4} & \frac{\partial Y}{\partial\lambda_5} \\ \frac{\partial\phi}{\partial\theta_1} & \frac{\partial\phi}{\partial\lambda_2} & \frac{\partial\phi}{\partial\lambda_3} & \frac{\partial\phi}{\partial\lambda_4} & \frac{\partial\phi}{\partial\lambda_5} \end{bmatrix} \tag{13} $$

$$ \begin{bmatrix} \dot{X} \\ \dot{Y} \\ \dot{\phi} \end{bmatrix} = J \begin{bmatrix} \dot{\theta_1} \\ \dot{\lambda_2} \\ \dot{\lambda_3} \\ \dot{\lambda_4} \\ \dot{\lambda_4} \end{bmatrix} \tag{14} $$

❖ DYNAMICS

$$ X_1 = L_1\cos(\theta_1) \tag{15} $$

$$ Y_1 = L_1\sin(\theta_1) \tag{16} $$

$$X_2 = L_1 \cos(\theta_1) + L_2 \cos(\theta_2) \quad (17)$$

$$Y_2 = L_1 \sin(\theta_1) + L_2 \sin(\theta_2) \quad (18)$$

$$X_3 = L_1 \cos(\theta_1) + L_2 \cos(\theta_2) + L_3 \cos(\theta_3) \quad (19)$$

$$Y_3 = L_1 \sin(\theta_1) + L_2 \sin(\theta_2) + L_3 \sin(\theta_3) \quad (20)$$

$$X_4 = L_1 \cos(\theta_1) + L_2 \cos(\theta_2) + L_3 \cos(\theta_3) + L_4 \cos(\theta_4) \quad (21)$$

$$Y_4 = L_1 \sin(\theta_1) + L_2 \sin(\theta_2) + L_3 \sin(\theta_3) + L_4 \sin(\theta_4) \quad (22)$$

$$X_5 = L_1 \cos(\theta_1) + L_2 \cos(\theta_2) + L_3 \cos(\theta_3) + L_4 \cos(\theta_4) + L_5 \cos(\theta_5) \quad (23)$$

$$Y_5 = L_1 \sin(\theta_1) + L_2 \sin(\theta_2) + L_3 \sin(\theta_3) + L_4 \sin(\theta_4) + L_5 \sin(\theta_5) \quad (24)$$

$$X_{1c} = L_{1c} \cos(\theta_1) \quad (25)$$

$$Y_{1c} = L_{1c} \sin(\theta_1) \quad (26)$$

$$X_{2c} = L_1 \cos(\theta_1) + L_{2c} \cos(\theta_2) \quad (27)$$

$$Y_{2c} = L_1 \sin(\theta_1) + L_{2c} \sin(\theta_2) \quad (28)$$

$$X_{3c} = L_1 \cos(\theta_1) + L_2 \cos(\theta_2) + L_{3c} \cos(\theta_3) \quad (29)$$

$$Y_{3c} = L_1 \sin(\theta_1) + L_2 \sin(\theta_2) + L_{3c} \sin(\theta_3) \quad (30)$$

$$X_{4c} = L_1 \cos(\theta_1) + L_2 \cos(\theta_2) + L_3 \cos(\theta_3) + L_{4c} \cos(\theta_4) \quad (31)$$

$$Y_{4c} = L_1 \sin(\theta_1) + L_2 \sin(\theta_2) + L_3 \sin(\theta_3) + L_{4c} \sin(\theta_4) \quad (32)$$

$$X_{5c} = L_1 \cos(\theta_1) + L_2 \cos(\theta_2) + L_3 \cos(\theta_3) + L_4 \cos(\theta_4) + L_{5c} \cos(\theta_5) \quad (33)$$

$$Y_{5c} = L_1 \sin(\theta_1) + L_2 \sin(\theta_2) + L_3 \sin(\theta_3) + L_4 \sin(\theta_4) + L_{5c} \sin(\theta_5) \quad (34)$$

The total kinetic energy (T) is,

$$T = \frac{1}{2} M_1 V_{1c}^2 + \frac{1}{2} M_2 V_{2c}^2 + \frac{1}{2} M_3 V_{3c}^2 + \frac{1}{2} M_4 V_{4c}^2 + \frac{1}{2} M_5 V_{5c}^2 + \frac{1}{2} I_1 \dot{\theta}_1^2 + \frac{1}{2} I_2 (\dot{\theta}_1 + \dot{\theta}_2)^2 + \frac{1}{2} I_3 (\dot{\theta}_1 + \dot{\theta}_2 + \dot{\theta}_3)^2 + \frac{1}{2} I_4 (\dot{\theta}_1 + \dot{\theta}_2 + \dot{\theta}_3 + \dot{\theta}_4)^2 + \frac{1}{2} I_5 (\dot{\theta}_1 + \dot{\theta}_2 + \dot{\theta}_3 + \dot{\theta}_4 + \dot{\theta}_5)^2 \quad (35)$$

The total potential energy (U) is,

$$U = M_1 g Y_{1c} + M_2 g Y_{2c} + M_3 g Y_{3c} + M_4 g Y_{4c} + M_5 g Y_{5c} \quad (36)$$

Lagrangian is the difference between total kinetic and total potential energy,

$$L = T - U \tag{37}$$

Lagrangian Mechanics equation is given as,

$$\tau_i = \frac{d\left(\frac{\partial L}{\partial \dot{q}}\right)}{dt} - \frac{\partial L}{\partial q}, where\ q\ is\ the\ parameter\ (i.e.\ \theta_1, \theta_2, \theta_3, \theta_4, \theta_5) \tag{38}$$

Joint torques upon solving the lagrangian mechanics equation is,

$$\tau_1 = [M_1 L_{1c}^2 + M_{25} L_1^2 + I_{15}]\ddot{\theta_1} + [(M_2 L_1 L_{2c} + M_{35} L_1 L_2) C_{12} + I_{23}]\ddot{\theta_2} + [(M_3 L_1 L_{3c} + M_{45} L_1 L_3) C_{13} + I_{35}]\ddot{\theta_3} + [(M_4 L_1 L_{4c} + M_5 L_1 L_4) C_{14} + I_{45}]\ddot{\theta_4} + [M_5 L_1 L_{5c} + I_5]\ddot{\theta_5} + gC_1[M_1 L_{1c} + M_{25} L_1] \tag{39}$$

$$\tau_2 = [(M_2 L_1 L_{2c} + M_{35} L_1 L_2)(C_{12} + S_{12}) + I_{25}]\ddot{\theta_1} + [M_2 L_{2c}^2 + M_{35} L_2^2 + I_{25}]\ddot{\theta_2} + [(M_3 L_2 L_{3c} + M_{45} L_2 L_3)(C_{23} + S_{23}) + I_{35}]\ddot{\theta_3} + [(M_4 L_1 L_{4c} + M_5 L_1 L_4)(C_{14} + S_{14}) + I_{45}]\ddot{\theta_4} + [(M_5 L_1 L_{5c})(C_{15} + S_{15}) + I_5]\ddot{\theta_5} - 2[M_2 L_1 L_{2c} + M_{35} L_1 L_2] S_{12} \dot{\theta_1} \dot{\theta_2} + gC_2[M_2 L_{2c} + M_{35} L_2] \tag{40}$$

$$\tau_3 = [(M_1 L_1 L_{3c} + M_{45} L_1 L_3)(C_{13} + S_{13}) + I_{35}]\ddot{\theta_1} + [(M_3 L_2 L_{3c} + M_{45} L_2 L_3)(C_{23} + S_{23}) + I_{35}]\ddot{\theta_2} + [M_3 L_{3c}^2 + M_{45} L_3^2 + I_{35}]\ddot{\theta_3} + [(M_4 L_3 L_{4c} + M_5 L_3 L_4)(C_{34} + S_{34}) + I_{45}]\ddot{\theta_4} + [(M_3 L_3 L_{5c})(C_{35} + S_{35}) + I_5]\ddot{\theta_5} - 2[M_3 L_1 L_{3c} + M_{45} L_1 L_3] S_{13} \dot{\theta_1} \dot{\theta_3} - 2[M_3 L_2 L_{3c} + M_{45} L_2 L_3] S_{23} \dot{\theta_2} \dot{\theta_3} + gC_3[M_3 L_{3c} + M_{45} L_3] \tag{41}$$

$$\tau_4 = [(M_4 L_1 L_{4c} + M_5 L_1 L_3)(C_{14} + S_{14}) + I_{45}]\ddot{\theta_1} + [(M_4 L_2 L_{4c} + M_5 L_2 L_4)(C_{24} + S_{24}) + I_{45}]\ddot{\theta_2} + [(M_4 L_3 L_{4c} + M_5 L_3 L_4)(C_{34} + S_{34}) + I_{45}]\ddot{\theta_3} + [M_4 L_{4c}^2 + M_5 L_4^2 + I_{45}]\ddot{\theta_4} + [(M_5 L_4 L_{5c})(C_{45} + S_{45}) + I_5]\ddot{\theta_5} - 2[M_4 L_1 L_{4c} + M_5 L_1 L_4] S_{14} \dot{\theta_1} \dot{\theta_4} - 2[M_4 L_2 L_{4c} + M_5 L_2 L_4] S_{24} \dot{\theta_2} \dot{\theta_4} - 2[M_4 L_3 L_{4c} + M_5 L_3 L_4] S_{34} \dot{\theta_3} \dot{\theta_4} + gC_4[M_4 L_{4c} + M_5 L_4] \tag{42}$$

$$\tau_5 = [(M_5 L_1 L_{5c})(C_{15} + S_{15}) + I_5]\ddot{\theta_1} + [(M_5 L_2 L_{5c})(C_{25} + S_{25}) + I_5]\ddot{\theta_2} + [(M_5 L_3 L_{5c})(C_{35} + S_{35}) + I_5]\ddot{\theta_3} + [(M_5 L_4 L_{5c})(C_{45} + S_{45}) + I_5]\ddot{\theta_4} + [(M_5 L_{5c}^2) + I_5]\ddot{\theta_5} - 2[M_5 L_1 L_{5c}] S_{14} \dot{\theta_1} \dot{\theta_5} - 2[M_5 L_2 L_{5c}] S_{25} \dot{\theta_2} \dot{\theta_5} - 2[M_5 L_3 L_{5c}] S_{35} \dot{\theta_3} \dot{\theta_5} - 2[M_5 L_4 L_{5c}] S_{45} \dot{\theta_4} \dot{\theta_5} + gC_5[M_5 L_{5c}] \tag{43}$$

The 5 torque equations can be represented in a more familiar matrix form as,

$$\begin{bmatrix}\tau_1\\ \tau_2\\ \tau_3\\ \tau_4\\ \tau_5\end{bmatrix}=\begin{bmatrix}M_{11} & M_{12} & M_{13} & M_{14} & M_{15}\\ M_{21} & M_{22} & M_{23} & M_{24} & M_{25}\\ M_{31} & M_{32} & M_{33} & M_{34} & M_{35}\\ M_{41} & M_{42} & M_{43} & M_{44} & M_{45}\\ M_{51} & M_{52} & M_{53} & M_{54} & M_{55}\end{bmatrix}\begin{bmatrix}\ddot{\theta}_1\\ \ddot{\theta}_2\\ \ddot{\theta}_3\\ \ddot{\theta}_4\\ \ddot{\theta}_5\end{bmatrix}+\begin{bmatrix}C_1\\ C_2\\ C_3\\ C_4\\ C_5\end{bmatrix}+\begin{bmatrix}G_1\\ G_2\\ G_3\\ G_4\\ G_5\end{bmatrix} \quad (44)$$

Where,

$$M_{11}=M_1L_{1c}^2+M_{25}L_1^2+I_{15} \quad (45)$$

$$M_{12}=(M_2L_1L_{2c}+M_{35}L_1L_2)C_{12}+I_{23} \quad (46)$$

$$M_{13}=(M_3L_1L_{3c}+M_{45}L_1L_3)C_{13}+I_{35} \quad (47)$$

$$M_{14}=(M_4L_1L_{4c}+M_5L_1L_4)C_{14}+I_{45} \quad (48)$$

$$M_{15}=M_5L_1L_{5c}+I_5 \quad (49)$$

$$M_{21}=(M_2L_1L_{2c}+M_{35}L_1L_2)(C_{12}+S_{12})+I_{25} \quad (50)$$

$$M_{22}=M_2L_{2c}^2+M_{35}L_2^2+I_{25} \quad (51)$$

$$M_{23}=(M_3L_2L_{3c}+M_{45}L_2L_3)(C_{23}+S_{23})+I_{35} \quad (52)$$

$$M_{24}=(M_4L_1L_{4c}+M_5L_1L_4)(C_{14}+S_{14})+I_{45} \quad (53)$$

$$M_{25}=(M_5L_1L_{5c})(C_{15}+S_{15})+I_5 \quad (54)$$

$$M_{31}=(M_1L_1L_{3c}+M_{45}L_1L_3)(C_{13}+S_{13})+I_{35} \quad (55)$$

$$M_{32}=(M_3L_2L_{3c}+M_{45}L_2L_3)(C_{23}+S_{23})+I_{35} \quad (56)$$

$$M_{33}=[M_3L_{3c}^2+M_{45}L_3^2+I_{35}]\ddot{\theta}_3 \quad (57)$$

$$M_{34}=(M_4L_3L_{4c}+M_5L_3L_4)(C_{34}+S_{34})+I_{45} \quad (58)$$

$$M_{35}=(M_3L_3L_{5c})(C_{35}+S_{35})+I_5 \quad (59)$$

$$M_{41}=(M_4L_1L_{4c}+M_5L_1L_3)(C_{14}+S_{14})+I_{45} \quad (60)$$

$$M_{42}=(M_4L_2L_{4c}+M_5L_2L_4)(C_{24}+S_{24})+I_{45} \quad (61)$$

$$M_{43}=(M_4L_3L_{4c}+M_5L_3L_4)(C_{34}+S_{34})+I_{45} \quad (62)$$

$$M_{44}=M_4L_{4c}^2+M_5L_4^2+I_{45} \quad (63)$$

$$M_{45}=(M_5L_4L_{5c})(C_{45}+S_{45})+I_5 \quad (64)$$

$$M_{51}=(M_5L_1L_{5c})(C_{15}+S_{15})+I_5 \quad (65)$$

$$M_{52}=(M_5L_2L_{5c})(C_{25}+S_{25})+I_5 \quad (66)$$

$$M_{53}=(M_5L_3L_{5c})(C_{35}+S_{35})+I_5 \quad (67)$$

$$M_{54}=M_4L_{4c}^2+M_5L_4^2+I_{45} \quad (68)$$

$$M_{55}=(M_5L_{5c}^2)+I_5 \quad (69$$

$$C_1=0 \quad (70)$$

$$C_2=[(M_5L_1L_{5c})(C_{15}+S_{15})+I_5]\ddot{\theta}_5-2[M_2L_1L_{2c}+M_{35}L_1L_2]S_{12}\dot{\theta}_1\dot{\theta}_2 \quad (71)$$

$$C_3=-2[M_3L_1L_{3c}+M_{45}L_1L_3]S_{13}\dot{\theta}_1\dot{\theta}_3-2[M_3L_2L_{3c}+M_{45}L_2L_3]S_{23}\dot{\theta}_2\dot{\theta}_3 \quad (72)$$

$$C_4 = -2[M_4L_1L_{4c} + M_5L_1L_4]S_{14}\dot{\theta}_1\dot{\theta}_4 - 2[M_4L_2L_{4c} + M_5L_2L_4]S_{24}\dot{\theta}_2\dot{\theta}_4 - 2[M_4L_3L_{4c} + M_5L_3L_4]S_{34}\dot{\theta}_3\dot{\theta}_4 \quad (73)$$

$$C_5 = -2[M_5L_1L_{5c}]S_{14}\dot{\theta}_1\dot{\theta}_5 - 2[M_5L_2L_{5c}]S_{25}\dot{\theta}_2\dot{\theta}_5 - 2[M_5L_3L_{5c}]S_{35}\dot{\theta}_3\dot{\theta}_5 - 2[M_5L_4L_{5c}]S_{45}\dot{\theta}_4\dot{\theta}_5 \quad (74)$$

$$G_1 = gC_1[M_1L_{1c} + M_{25}L_1] \quad (75)$$

$$G_2 = gC_2[M_2L_{2c} + M_{35}L_2] \quad (76)$$

$$G_3 = gC_3[M_3L_{3c} + M_{45}L_3] \quad (77)$$

$$G_4 = gC_4[M_4L_{4c} + M_5L_4] \quad (78)$$

$$G_5 = gC_5[M_5L_{5c}] \quad (79)$$

Additional term J^TF can be added to the right-hand side (RHS) of the eqn. (44) to account for external load acting on the hand of the body to account for the load lifted during performing a task.

3.3 ROBOT KINEMATIC AND DYNAMICS

The exoskeleton in the current study has active motion only in the sagittal plane. It is ensured that it does not block or restrict any of the body's motion in other planes (i.e., coronal and transverse plane). The dynamics of the robot give the information as to mimic the behaviour of a real world/practical system. It is useful tool for simulating and designing a controller for the exoskeleton.

TABLE 18 : PARAMETERS AND SYMBOLS USED IN SEC. 3.3 (eqn. (80) to eqn. (91))

S.No.	PARAMETER	UNITS	DESCRIPTION
1	θ_1	Degree ($^\circ$)	Angle of rotation of Link 1 wrt. horizontal
2	$\dot{\theta_1}$	rad./s	Angular Velocity of Link 1
3	$\ddot{\theta_1}$	Rad./s^2	Angular Acceleration of Link 1
4	R_z	-	Rotational Matrix for rotation about z-axis
5	X	m	X axis co-ordinate of end effector (tip of Link 1)

6	Y	m	Y axis co-ordinate of end effector (tip of Link 1)
7	X_c	m	X axis co-ordinate of centroid of Link 1
8	Y_c	m	Y axis co-ordinate of centroid of Link 1
9	L_1	m	Length of Link 1
10	L_{1c}	m	Length of centroid of Link 1 from origin (i.e., base of Link 1)
11	I_1	Kg-m^2	Moment of Inertia of Link 1 about its centroid
12	L	-	Lagrangian
13	T	Kg-m^2/s	Total Kinetic Energy
14	U	Kg-m^2/s	Total Potential Energy
15	τ_1	N-m	Toque at joint 1

A. LUMBAR/WAIST EXOSKELETON

The dynamics equation of the robot can be expressed as a 1 DOF planar rotary robot. The mass of the robot is approximately estimated considering the link material to be carbon fibre which has a density of about 1800 Kg/m^3. It has a Young's modulus of about 228 GPa and ultimate tensile strength of 3.5 GPa.

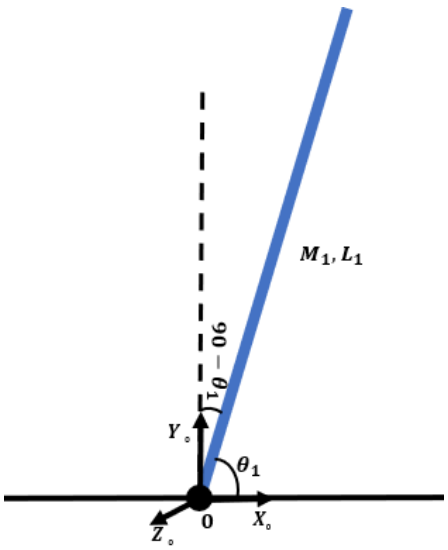

Fig. 8 : REPRESENTATION OF 1 DOF EXOSKELETON ROBT

❖ KINEMATICS

The selected lumbar/waist exoskeleton for the study has 1 DOF thus there is no need for writing its DH parameters as the robot is a simple planar rotary joint robot with no singularity.

The robot's end co-ordinates can be expressed in joint co-ordinate by directly measuring the angle θ_1 while to convert it into cartesian co-ordinates it is simply multiplied with a rotation matrix given about z-axis (it is convention to assume that the rotation is about z-axis).

The robots base about which it pivots is considered as the origin and θ_1 is the angle that the robot's link makes with the horizontal.

$$R_z = \begin{bmatrix} \cos(\theta_1) & -\sin(\theta_1) & 0 \\ \sin(\theta_1) & \cos(\theta_1) & 0 \\ 0 & 0 & 1 \end{bmatrix} \quad (80)$$

$P = \begin{bmatrix} X \\ Y \\ 0 \end{bmatrix}$, P is the co-ordinate of the robots end at home position (81)

$P' = R_z P$, P' is the new co-ordinate of the robots end after it moves to make an angle of θ_1 with the horizontal. (82)

❖ DYNAMICS

$$X = L_1 \cos(\theta_1) \quad (83)$$

$$Y = L_1 \sin(\theta_1) \quad (84)$$

$$X_c = L_{1c} \cos(\theta_1) \quad (85)$$

$$Y_c = L_{1c} \sin(\theta_1) \quad (86)$$

The total kinetic energy (T) of the robot is,

$$T = \frac{1}{2} I_1 \dot{\theta}_1^2 + \frac{1}{2} M_1 L_{1c}^2 \dot{\theta}_1^2 \quad (87)$$

The total Potential energy (T) of the robot is,

$$U = M_1 g Y_{1c} \quad (88)$$

Lagrangian is the difference between total kinetic and total potential energy,

$$L = T - U \quad (89)$$

Lagrangian Mechanics equation is given as,

$$\tau_i = \frac{d\left(\frac{\partial L}{\partial \dot{q}}\right)}{dt} - \frac{\partial L}{\partial q}, where\ q\ is\ the\ parameter\ (i.e.\ \theta_1) \quad (90)$$

Joint torque upon solving the lagrangian mechanics equation is,

$$\tau_1 = [I_1 + M_1 L_{1c}^2]\ddot{\theta}_1 - M_1 g L_{1c} \cos(\theta_1) \quad (91)$$

Additional term $J^T F$ can be added to the right-hand side (RHS) of the eqn. (91) to account for external load acting on the end effector (tip of the robot)

B. ELBOW EXOSKELETON

The elbow joint is simple and not complex 1 DOF joint thus the exoskeleton for this joint is taken as 1 DOF, which is the same as lumbar/the lumbar/waist exoskeleton robot.

The kinematic and dynamic equation of elbow and lumbar/waist exoskeleton is exactly the same as both are 1 DOF planar robots (i.e., Ch.3, Sec. 3.3, A). The only difference is the mass, moment of inertia and the location of centre of mass.

3.4 MOTOR DYNAMICS

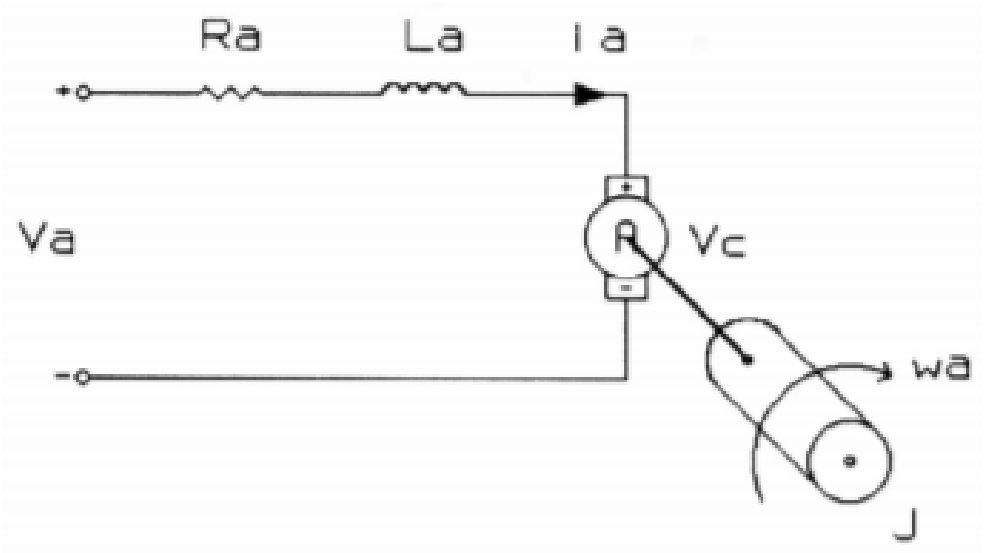

Fig. 9 : REPRESENTATION OF MOTOR
BY -Mulka, Viplav. (2016). Hardware in the Loop architecture for a DC Motor. 10.13140/RG.2.2.30480.40962.)

TABLE 19 : PARAMETERS AND SYMBOLS USED IN SEC. 3.4 (eqn. (105) to eqn. (116))

S.No.	PARAMETER	UNITS	DESCRIPTION
1	V_a	Volts (V)	Voltage Source-across armature coil
2	V_{Ra}	Volts (V)	Voltage across Resistance
3	V_{La}	Volts (V)	Voltage across inductor
4	V_c	Volts	Back emf
5	i_a	A	Current through the armature coil
6	K_v	-	Speed/Velocity Constant
6	ω_a	RPM	Rotational Velocity of armature

7	J	Kg-m^2	Rotor Inertia
8	B	N-s/m = Kg/s	Damping Coefficient
9	L_a	H	Inductance due to armature coil in series
10	K_t	-	Torque Constant
11	T_e	N-m	Electromagnetic Torque
12	$T_{\omega 1}$	N-m	Torque due to rotational acceleration of the rotor
13	T_ω	N-m	Torque due to rotational Velocity of the rotor
14	T_L	N-m	Torque due to mechanical load
15	$I_a(s)$	-	Laplace transform of i_a
16	$\Omega_a(s)$	-	Laplace transform of ω_a
17	$V_a(s)$	-	Laplace transform of V_a
18	$T_L(s)$	-	Laplace transform of T_L
19	R_a	Ω	Resistance due to armature coil

A. ELECTRICAL CHARACTERISTICS

Applying Kirchhoff's law to balance the voltages across the circuit,

$$V_a - V_{Ra} - V_{La} - V_c = 0 \quad (105)$$

$$V_{Ra} = I_a R_a \quad (106)$$

$$V_{La} = L_a \frac{di_a}{dt} \quad (107)$$

$$V_c = K_v \omega_a \quad (108)$$

Substituting eqn. (103) to eqn. (105) into eqn. (106),

$$V_a - i_a R_a - L_a \frac{di_a}{dt} - K_v \omega_a = 0 \quad (109)$$

B. MECHANICAL CHARACTERISTICS

Balancing torques,

$$T_e - T_{\omega 1} - T_\omega - T_L = 0 \quad (110)$$

$$T_e = K_t i_a \quad (111)$$

$$T_{\omega 1} = J\frac{d\omega_a}{dt} \quad (112)$$

$$T_\omega = B\omega_a \quad (113)$$

Substituting eqn. (108) to eqn. (110) into eqn. (111),

$$K_t i_a - J\frac{d\omega_a}{dt} - B\omega_a - T_L = 0 \quad (114)$$

C. TRANSFER FUNCTION

Taking Laplace transform of eqn. (109)

$$sI_a(s) - i_a(0) = -\frac{R_a}{L_a}I_a(s) - \frac{K_v}{L_a}\Omega_a(s) + \frac{1}{L_a}V_a(s) \quad (115)$$

Taking Laplace transform of eqn. (114),

$$s\Omega_a(s) - \omega_a(0) = \frac{K_t}{J}I_a(s) - \frac{B}{J}\Omega_a(s) - \frac{1}{J}T_L(s) \quad (116)$$

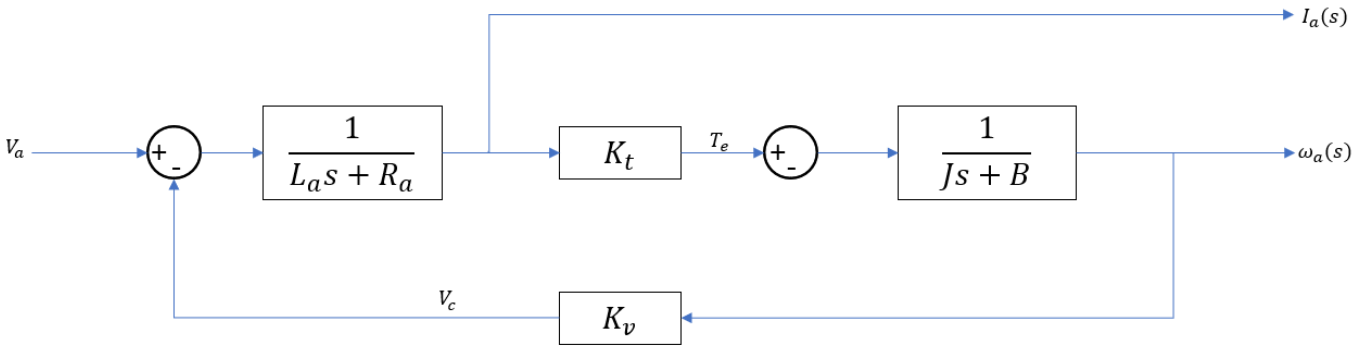

Fig. 10 : FLOW DIAGRAM REPRESENTATION OF DC MOTOR USING TRANSFER FUNCTION

3.5 MOTOR-EXOSKELETON COMBINED DYNAMICS – 1 DOF

The motor is connected to the exoskeleton joint through a gear reducer whose value was decided in Section 2.4. The gear ratio is the ratio of input speed to output speed or input torque to output torque. From this relation the motor's output torque and speed can be found which is the exoskeletons input torque thus the equation is modified only in the mass matrix as,

$$\left[\frac{I_1}{GR^2} + M_1 L_{1c}^2 + J\right]\ddot{\theta}_1 \quad (117)$$

In addition to this an additional term B is added to the entire expression.

Thus, the complete dynamics equation for 1 DOF exoskeleton with motor and gear ratio is represented as,

$$\tau_1 = \left[\frac{I_1}{GR^2} + M_1 L_{1c}^2 + J\right]\ddot{\theta}_1 - M_1 g L_{1c}\cos(\theta_1) + B \quad (118)$$

3.6 HUMAN-EXOSKELETON INTERACTION MODEL

The human machine interaction model is of importance if sensor is being used to find the exoskeleton end-effector forces that is used to control and provide assistance.

The pressure sensor that is being used produces an output voltage when a force/pressure is applied on it, examples of it include strain gauge, piezoelectric materials, etc Most commercially available pressure sensor (push-pull type) have linear relation between the applied pressure and output voltage thus it is not of primary concern to find the pressure-voltage relation as it will only affect proportional part of the controller whose value can be easily adjusted if the pressure-voltage relation is not in the ratio 1:1.

For the current study a ratio of 1:1 is assumed and is a give thus forth.

Human-exoskeleton interaction that produces the interaction forces can be simplified and visualized as a spring-damper system.

The relation between linear spring-damper system and joint angle (based on the assumption that the tracking error is very less) is given as,

$$\Delta d_1 \approx l_1 \Delta\theta_1 \quad (119)$$

$$\Delta d_2 \approx 2l_1 \Delta\theta_1 + l_2 \Delta\theta_2 \quad (120)$$

$$\Delta d_3 \approx 2l_1 \Delta\theta_1 + 2l_2 \Delta\theta_2 + l_3 \Delta\theta_3 \quad (121)$$

$$\Delta d_4 \approx 2l_1 \Delta\theta_1 + 2l_2 \Delta\theta_2 + 2l_3 \Delta\theta_3 + l_4 \Delta\theta_4 \quad (122)$$

$$\Delta d_5 \approx 2l_1 \Delta\theta_1 + 2l_2 \Delta\theta_2 + 2l_3 \Delta\theta_3 + l_4 \Delta\theta_4 + l_5 \Delta\theta_5 \quad (123)$$

The eqn. (119) to eqn. (123) represents the relation between joint angles and linear displacement of spring (not limited by the exoskeleton DOF). The subscript represents the link number and l_1. l_2. l_3. l_4. l_5 are the length where the sensor is located which is taken as the centre of the links for the current study.

For 1 DOF exoskeleton only $\Delta d_1$is used, for 3 DOF exoskeleton $\Delta d_1, \Delta d_2, \Delta d_3$are used and $d_1, \Delta d_2, \Delta d_3, \Delta d_4, \Delta d_5$ are used in case of 5 DOF exoskeleton.

The interaction force (F_i) for a given link i is given by,

$$F_i = k\Delta d_i + b\Delta d_i$$

Where, k is the stiffness and b is the damping coefficient of the human body. The value of the stiffness constant (k) and damping coefficient (b) is taken as 1 N-m/m and 8 N-m-s/m is taken [38]. These values are used henceforth in the current study.

CHAPTER 4

4.1 INTRODUCTION

This chapter discusses the various control strategies and implementation for application in upper body exoskeleton, particularly for elbow and lumbar/waist joints. The level of interaction between the robot and human decides its versatility and usage. The control system implementation in a virtual environment/simulation allows to check and modify the behaviour of the robot by controlling various parameters.

The implementation of control system allows for reduced error in movement of the joints and applied torques also helps achieve a steady state response faster by tuning the parameters.

There are various control system strategies that are used for the control of exoskeleton however the one discussed here is based on model control. This control strategy was employed in the BLEEX [6] robot. PID, PD and PI controllers are most popularly used for the control of the exoskeleton. This however also has a its limitations as a linear controller are used to control a non-linear system.

4.2 VARIOUS CONTROL STRATEGIES

The various control strategies that are used to control the exoskeleton is classified as, model based, hierarchy based, physical parameter based and usage based. Fig. 11 shows the classification and sub-classification of these control strategies that will be discussed in this section.

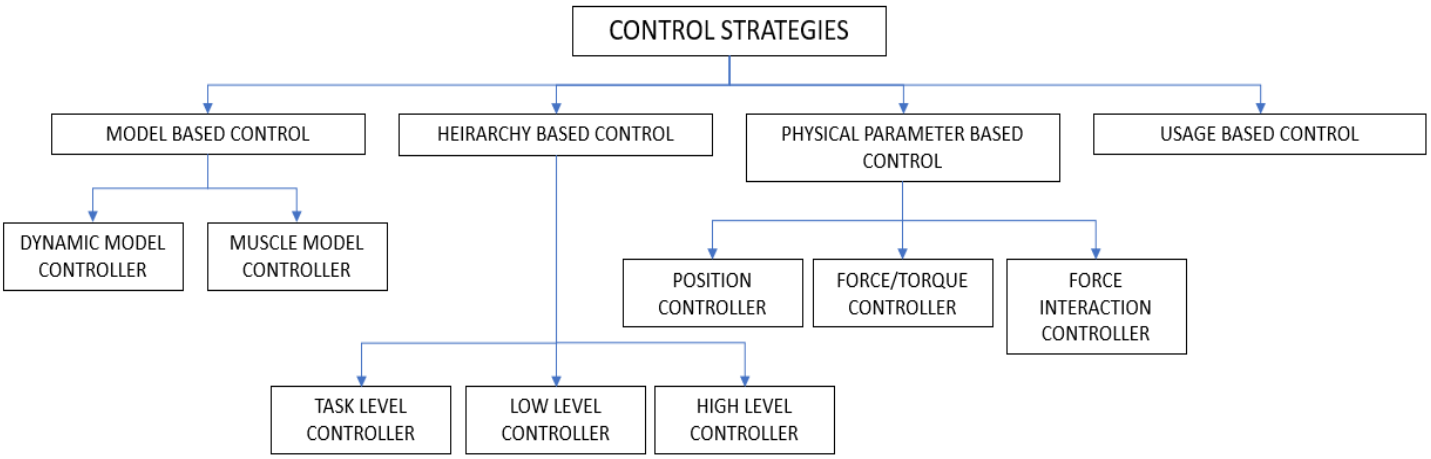

Fig. 11 : VARIOUS CONTROL STRATEGIES

A. MODEL BASED CONTROL

The model-based control is further sub-divided into 2, dynamic model and muscle model.

The muscle model establishes relation between input joint angles and muscle activation to output forces.

The exoskeleton model used for the current study is the dynamic model (mathematical modelling) and is thus only discussed in this section. The dynamic model is used to determine the relation between input and output that is joint torque and joint positions.

The various methods used to find the dynamic model are-

- **MATHEMATICAL MODELLING** –
  - It was used by BLEEX [6] exoskeleton to find the mathematical model for various phases of walking
  - The model needs to be precise in order to perform well.
  - Various methods such as Lagrangian mechanics, Newton-Euler method, etc. are used for its derivation.
- **SYSTEM IDENTIFICATION**
  - It was used by BLEEX [6] exoskeleton to control the swing phase of the leg (least squared method was implemented)
  - It is used when it is difficult to get good representation of the dynamic model by mathematical modelling
- **ARTIFICIAL INTELLIGENCE METHOD**
  - It is popularly used to identify complex non-linear systems.
  - Wavelet neural network was used to identify the dynamic model (torque output corresponding to input of position, velocity and acceleration) of exoskeleton by Xiuxia[26]

B. HEIRARCHY BASED CONTROL

The hierarchy-based control is sub-divided into 3 based on the hierarchy level as-

- **TASK LEVEL**
  - It is the highest-level controller
  - It is used to assign various controllers bases on the type of task being performed
- **HIGH LEVEL**
  - It receives information from the task level controller
  - It is used to control the human-exoskeleton interaction forces
- **LOW LEVEL**
  - It is the lowest level controller
  - It is responsible for controlling the joint position or torque/force of the exoskeleton.

C. PHYSICAL PARAMETER BASED CONTROL

It is a classification that is based on the physical parameters that is being controlled and is sub-divided into 3 as-

- **POSITION CONTROLLER**
  - It is a low-level controller
  - It is used to ensure that the exoskeleton's joint angle is the same as the human limb's joint angle (as measured by IMU sensor)
  - Example of it is the low-level PD controller used in ARMIN III [26] (arm exoskeleton used for medical rehabilitation)
  - HAL [14] also implemented PD position controller
- **TORQUE/FORCE CONTROLLER**
  - It is generally used as a low-level controller
  - It is used to ensure that the exoskeleton's joint torque is controlled to produce the desired human-exoskeleton interaction force.
  - Example of exoskeleton using this type or controller are ARMIN III [26]
- **FORCE INTERACTION CONTROLLER**
  - It is used as a high-level controller. Its aim is to provide necessary assistance during a task.
  - The interaction force can be controlled either by using impedance (input is position and the output is force/torque) or admittance control (input is force/torque and the output is position).
  - Impedance controller receives error in joint position to give force/torque that acts as a reference for the force/torque controller.
  - Admittance controller receives error in force/torque to give joint positions that acts as a reference for the position controller.
- Usually impedance/admittance controller is used provided the parameters are fixed however sometimes the parameters themselves may change due to external changes thus there may be a need for adaptive controllers such as fuzzy PID, etc.

D. USAGE BASED CONTROL

This classification is based on the usage of the designed exoskeleton such as GAIT controller (based on the gait task selects the control strategy), tele-operated controller (master-slave control, that is a separate external robot will shadow the *movements* of the operator), etc.

4.3 PID TUNING METHOD

The main objective of tuning PID parameters is to ensure that the plant is able to maintain set-point value and reach it as fast as possible (usually) all while ensuring minimum accepted level of error (ideally it should be zero).

The PID is widely accepted for use in exoskeletons where the aim is to track the joint and provide assistance. The tuning of PID is of extreme importance is exoskeletons as it requires to track the human motion and for it to be effective it should have a very low response time and very low error. The overshoot/undershot percentage that is acceptable for exoskeletons is also very low as high overshoot can be detrimental to the health of the wearer.

There are various methods of tuning a PID, however in this section we will limit our scope to Genetic algorithm for non-linear systems, particularly for elbow and waist/lumbar exoskeletons.

❖ GENETIC ALGORITHM (GA) PID

It is a search-based optimization technique based on the concepts of natural selection and genetics. It is one of the most popular and widely used method to find optimal solution to problems such as tuning a PID.

The algorithm works by initializes a random population (chromosomes) at first whose fitness value is evaluated based on an objective function (eg. Integral of absolute error). The simulation terminates if the fitness function is within a pre-defined set criterion else, a set of parents are selected at random to produce offspring which are generated using single point or multi point criteria (it can be compared to structured shuffling). The offspring are then randomly mutated (i.e., 1 change to 0 and vice versa for a 2-bit type approach to the problem). The new mutated population now becomes the initial population and the entire process repeats until the solution terminates or the set number of iterations are completed.

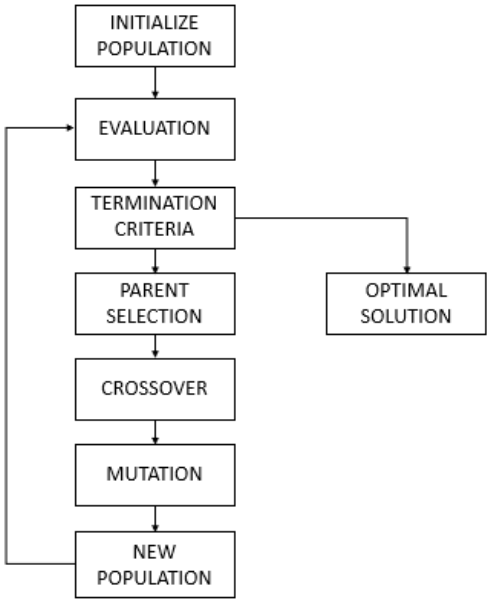

Fig. 12 : WORK FLOW OF GENETIC ALGORITHM

The code used for tuning of PID parameters using genetic algorithm is mentioned below,

```
open('THREE_PID.slx')
load('ELBOW_prop..mat')

%% PROBLEM DEFINATION
objfun = @(K)control_ga(K);

global K_p K_i K_d %K_p1 K_i1 K_p2 K_i2

N = 2;

K_min = [0 0 0 0 0 0];
K_max = [30 15 5 5 15 10]; %  [10 500 10 10 500 10 500];

%% GA PARAMETER INITILIZATION

popsize = 200;
MaxIt = 100;

nb = [20 20 20 20 20 20];%[20 23 20 20 23 20 23];
Nt = sum(nb);

selection_rate = 0.25 % probability of selection
mutation_rate = 0.1 % probability of mutation

total_mutations = floor(mutation_rate*Nt*popsize);

%% POPULATION INITIALIZATION

initialpop = round(rand(popsize,Nt))

a = 0; % variable representing the starting point of sub-string
b = 0;% variable representing the ending point of sub-string

for i =1:N
    a = b +1;
    b = b + nb(i);

    DV = bi2de(initialpop(:,(a:b)));
    K(:,i) = K_min(i) + (((K_max(i) - K_min(i))*DV)/(2^nb(i) - 1));
end

%% FITNESS EVALUATION

for i = 1:popsize

    K_p = K(i,1);
    K_i = K(i,2);
%     K_d = K(i,3);
    sim('THREE_PID') % running model from script*
    ch1 = ans.ISE1(end)
    ch2 = ans.ISE1(end)
    ch3 = ans.ISE1(end)
```

```
    ch = [ch1,ch2,ch3]
    fit(i,3) = (ch); % objfun(K(i,:));
    fitness(i,3) = 1./(1+fit(i,3));

end

%% selection of mating pool
for ii = 1:MaxIt
    fitprob = fitness./sum(fitness);
    cumprob = cumsum(fitprob);

    for i = 1:popsize
        r = rand(1,3);
        for j = 1:popsize
            if r < cumprob(j,1:3)
                newpop(i,:) = initialpop(j,:);
                break
            end
        end
    end

    %% PARENT SELECTION

    l = 0; % index for parent matrix
    m = 0; % index for remaining population matrix

    Parent = []; % initializing parent matrix
    rempop = []; % initializing remaining popultaion matrix for those who
were not selected as parent

    for k = 1:popsize
        R = rand;
        if R < selection_rate
            l = l+1;
            Parent(l,:) = newpop(k,:);
        else
            m = m+1;
            rempop(m,:) = newpop(k,:);
        end
    end


%% CROSSOVER
offspring = []; % initializing offspring matrix

if size(Parent,1) > 1
    for i = (size(Parent,1)-1)
        r = randi(Nt);
        offspring(i,:) = [Parent(i,1:r) Parent(i+1,r+1:Nt)];
    end
    r = randi(Nt);
    offspring(i+1,:) = [Parent(i+1,1:r) Parent(1,r+1:Nt)];
    newpop = [offspring;rempop];
end
```

```
%% MUTATIONS

totgen = popsize*Nt;

for i = 1:total_mutations
    r = randi(totgen);

    row = (ceil(r/Nt));

    if rem(r,Nt) == 0
       col = Nt;
    else
        col = rem(r,Nt);
    end

    if newpop(row,col) == 1
       newpop(row,col) = 0
    else
        newpop(row,col) = 1
    end
end

%% FITNESS EVALUATION OF NEW POPULATION

a = 0;
b = 0;

for i = 1:N
    a = b+1;
    b = b+nb(i);
    DV = bi2de(newpop(:,(a:b)));
    K(:,i) = K_min(i) + ((K_max(i) - K_min(i))*DV)/(2^nb(i) - 1);

end

for i = 1:popsize
    K_p = K(i,1);
    K_i = K(i,2);
%     K_d = K(i,3);
    sim('THREE_PID') % running model from script*
    ch1 = ans.ISE1(end)
    ch2 = ans.ISE1(end)
    ch3 = ans.ISE1(end)
    ch = [ch1,ch2,ch3]
    fit(i,3) = (ch); % objfun(K(i,:));
    fitness(i,3) = 1./(1+fit(i,3));

end

initialpop = newpop;
end
```

4.4 IMPLEMENTATION AND RESULTS

In this section the Simulink model of the elbow and lumbar/waist exoskeleton and its control using GA-PID is evaluated and compared for the tracking and assistance problem. The control architecture for the exoskeletons is shown in fig. 13. It has 3 PI controller (voltage controller, current controller, force controller). The Simulink model is designed in order to provide complete assistance to the human, that is the entire load is supported by the exoskeleton.

The pressure sensor and voltage relation is taken as linear and directly proportional to voltage, however any other value can also be used without affecting the controller performance (minor modifications in P value of the force controller) as it is essentially a proportional gain.

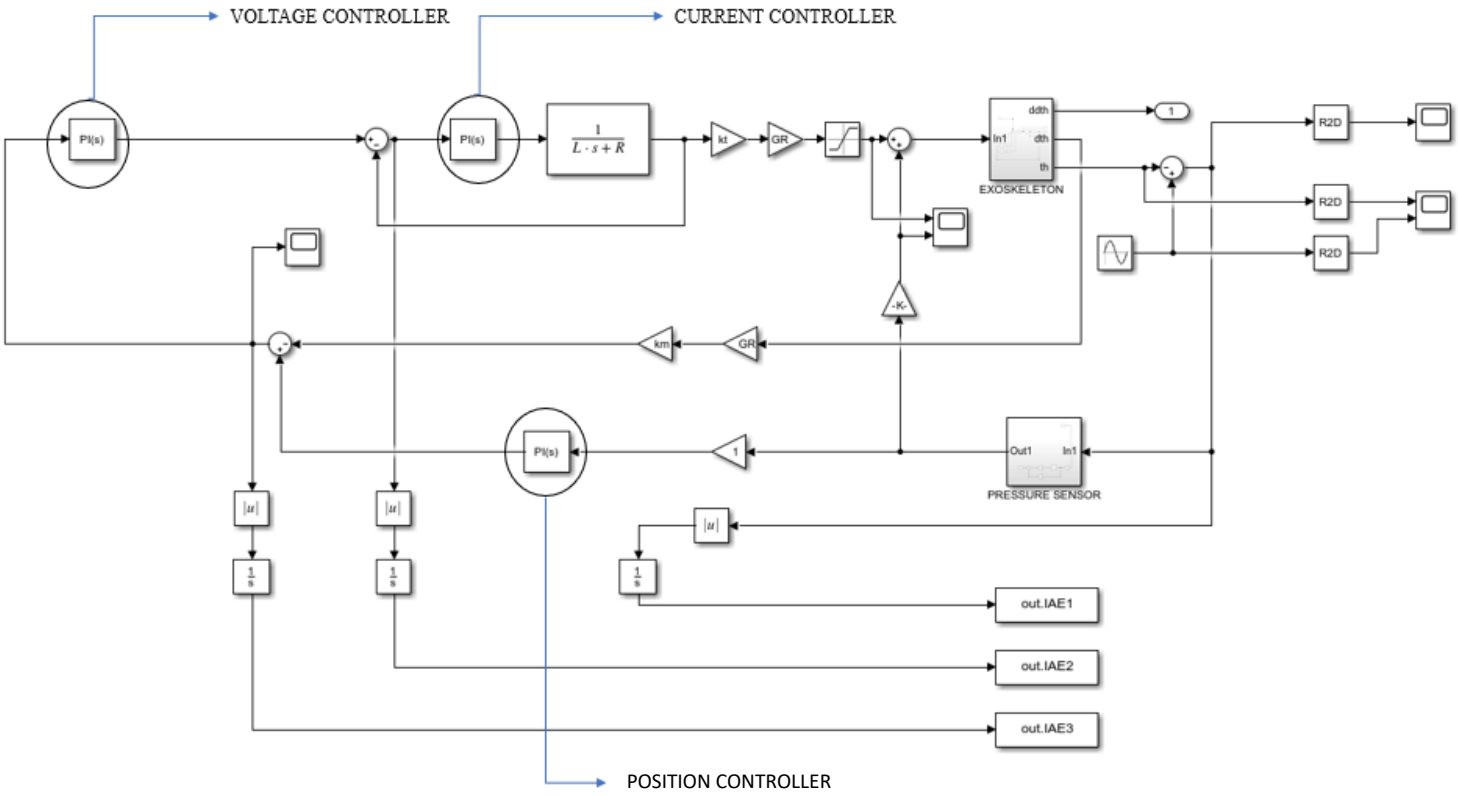

Fig. 13 : CONTROL ARCHITECHTURE : ELBOW AND LUMBAR EXOSKLETON

❖ GENETIC ALGORITHM (GA) – PID

The control structure has a total of 3 PI controller thus making it a multi-objective problem in which 3 objective functions need to be reduced in order to give the best fitness value (least). This is achieved by passing the objective function as a vector which in this case is taken as integral absolute error (IAE).

The stopping criteria was set as 50 generation (stall generation) and the simulation was run for a maximum of 100 generation with population size of 200.

The pareto chart is plotted in 3D space which gives list of best possible outcomes from which one is selected that closely satisfy the needs and purpose of the controller (minimum position error and no or low amplitude chattering in torque profile).

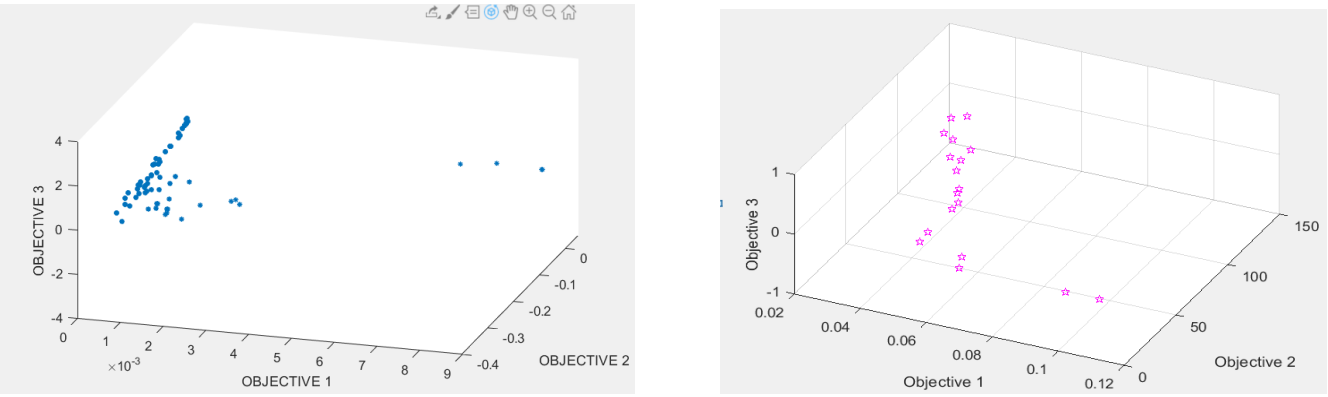

(a) ELBOW EXOSKELEON **(b) LUMBAR/WAIST EXOSKELETON**

Fig. 14: PARETO CHART

The data for pareto chart was analysed to make best decision for the 6 parameters to ensure minimal tracking error and the minimum torque by human.

The parameter values for the 3 PI controller with 17 Kg external load is given in TABLE 21. These value of parameters for PI are used for all the 3-test load (17Kg, 22.6 Kg and 29 Kg) cases of experimental gait and for no load-condition as mentioned in the previous chapters.

TABLE 20: TUNED PARAMETERS OF CONTROLLER USING GENETIC ALGORITHM

: ELBOW AND LUMBAR/WAIST EXOSKELETON

	S.No.	PARAMETER	VALUE	DESCRIPTION
ELBOW EXOSKELETON	**1**	K_p	29.82850	PI – Position controller
	2	Ki	7.062367	
	3	K_{p1}	0.0527	PI – Voltage controller
	4	Ki_1	0.9584	
	5	K_{p2}	10.5218	PI – Current controller
	6	Ki_2	7.4620	
LUMBAR/WAIST EXOSKELETON	**7**	K_p	39.49597	PI – Position controller
	8	Ki	8.297561	
	9	K_{p1}	0.6431004	PI – Voltage controller
	10	Ki_1	1.346280	
	11	K_{p2}	12.93314	PI – Current controller
	12	Ki_2	8.856908	

The tracking response of 1-DOF exoskeleton for all the load cases is given from fig. 16 to fig. 23. Each case has 2 figures giving the joint tracking and the actuator torque required.

The desired input tracking trajectory input is given as a sinusoidal wave of 0.4 rad (22.92 degrees) amplitude and 2 rad/s (114.59 degrees/s) frequency.

The external torque disturbance of frequency 10 Hz/62.8 rad/s (as the frequency of slight human tremor ranges from 6-12 Hz) is given with an amplitude of 3 degrees/0.0523599 radians.

A. ELBOW EXOSKELETON

All the data is taken and compiled in TABLE 20 from previous sections that are useful in designing and simulating the exoskeleton controller.

The data compiled in TABLE 21 is used hence forth for elbow exoskeleton.

TABLE 21: DATA USED FOR DESIGNING CONTROLLER FOR ELBOW EXOSKELETON

S.No.	PARAMETER	DESCRIPTION	UNITS	VALUE
1	J_{exo_elbow}	Moment of Inertia of exoskeleton	Kg-m^2	0.0396
2	J_{motor}	Moment of Inertia of motor	Kg-m^2	0.000306
3	M_{motor}	Mass of motor	Kg	0.6
4	M_{exo_elbow}	Mass of exoskeleton	Kg	1.5
5	L_{exo_elbow}	Length of exoskeleton link	m	0.3250
6	K_v	Speed/Velocity Constant	V-s/m	0.272
7	K_t	Torque Constant	N-m/A	0.217
8	L	Motor Inductance	H	0.0025
9	R	Motor Resistance	Ω	2.28
10	GR	Gear Ratio	-	200

The maximum error in tracking angle with and without the disturbance signal for all the test cases as that of the experimental data is compiled in TABLE 22. The error in tracking is well within acceptable limits thus, the controller is not just robust but also has good response time.

TABLE 22: MAXIMUM POSITION TRACKING ERROR FOR GA TUNED PARAMETERS OF CONTROLLER : ELBOW AND LUMBAR/WAIST EXOSKELETON

	NO DISTURBANCE				EXTERNAL DISTURBANCE			
LOAD	**No Load**	**17 Kg**	**22.6 Kg**	**29 Kg**	**No Load**	**17 Kg**	**22.6 Kg**	**29 Kg**
ELBOW EXOSKELETON: Maximum Error (degrees)	1.122	0.4178	0.4285	0.9125	1.048	0.361	0.483	1.282

NOTE – The maximum error in angle occurs during the sencond cycle of the sine wave at a time of roughly 2.5 seconds. The error for the first cycle is significantly smaller lying under 1 degree. This scenario will not occur in practical cases usually, however the error is still within acceptable limits

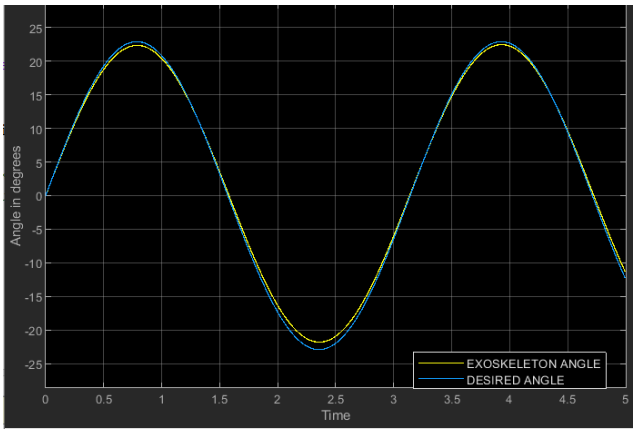

(a) TRACKING RESPONSE : NO LOAD

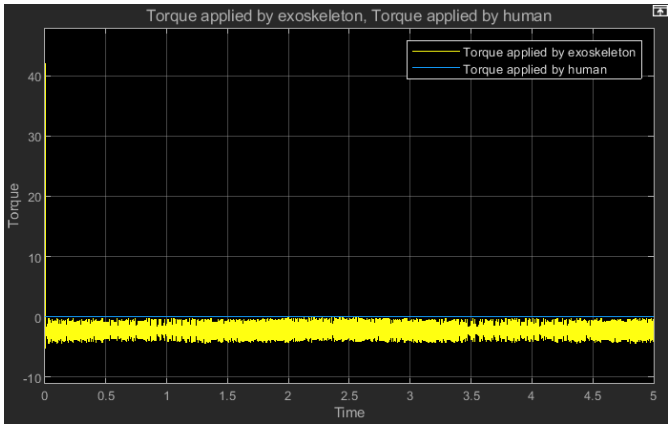

(b) TORQUE PROFILE: NO LOAD

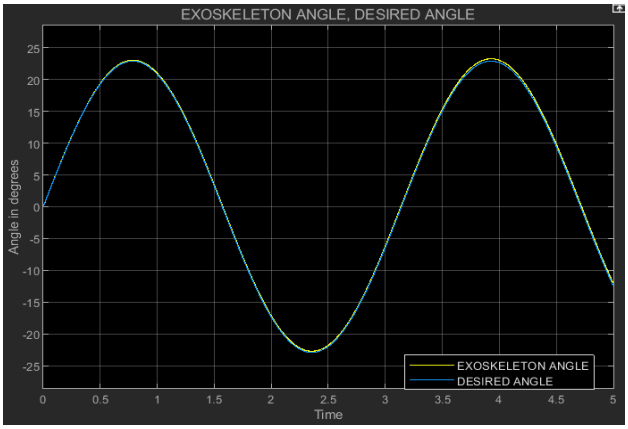

(c) TRACKING RESPONSE : 17 Kg LOAD

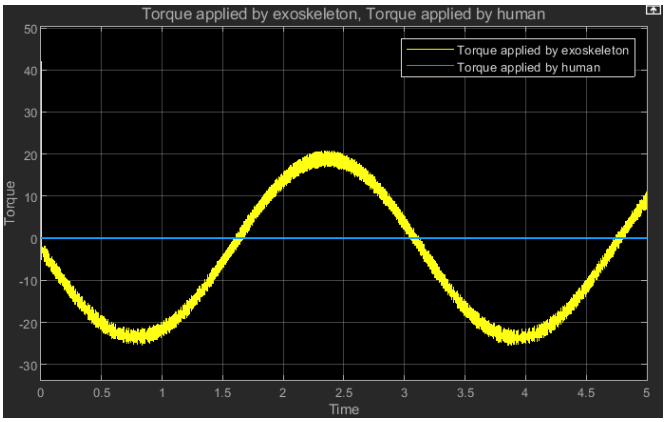

(d) TORQUE PROFILE: 17 Kg LOAD

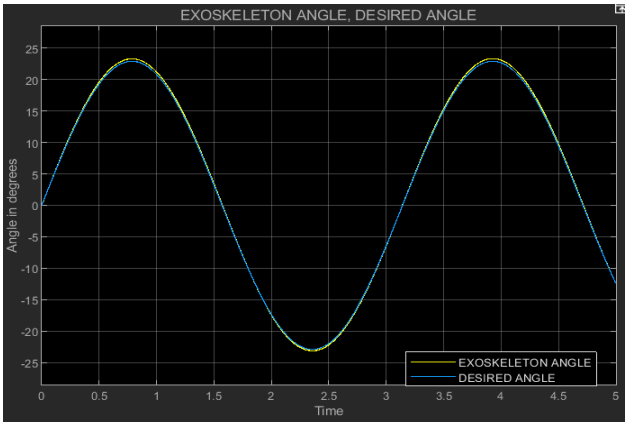

(e) TRACKING RESPONSE : 22.6 Kg LOAD

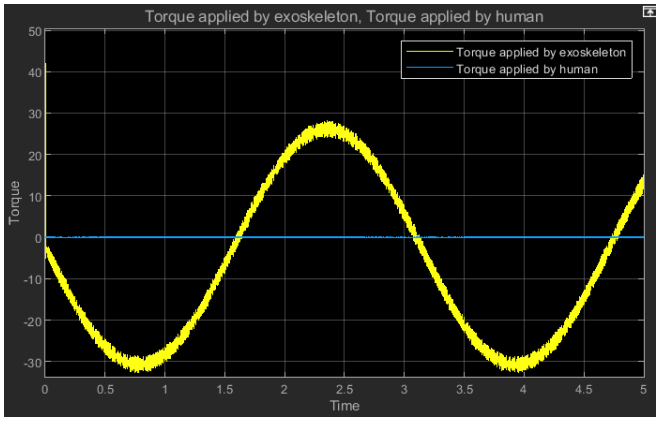

(f) TORQUE PROFILE: 22.6 Kg LOAD

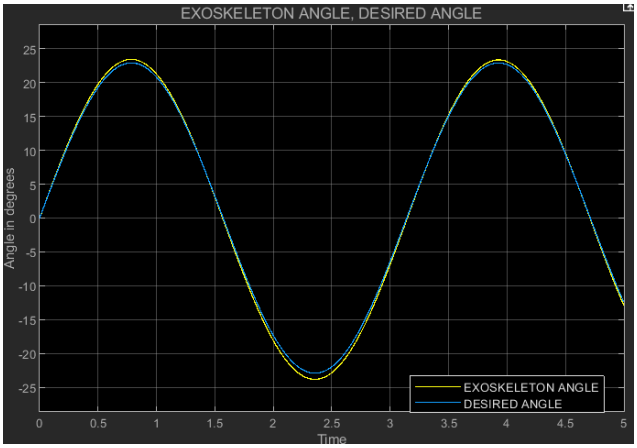

(g) TRACKING RESPONSE : 22.6 Kg LOAD

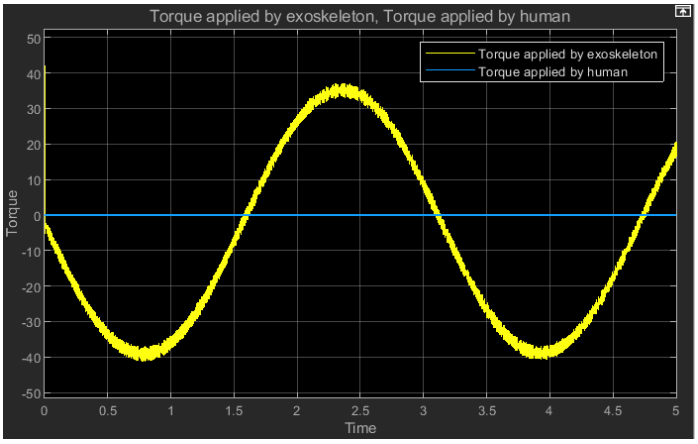

(h) TORQUE PROFILE: 22.6 Kg LOAD

Fig. 15 : TRACKING AND TORQUE OF ELBOW EXOSKELETON IN ABSENCE OF DISTURBANCE

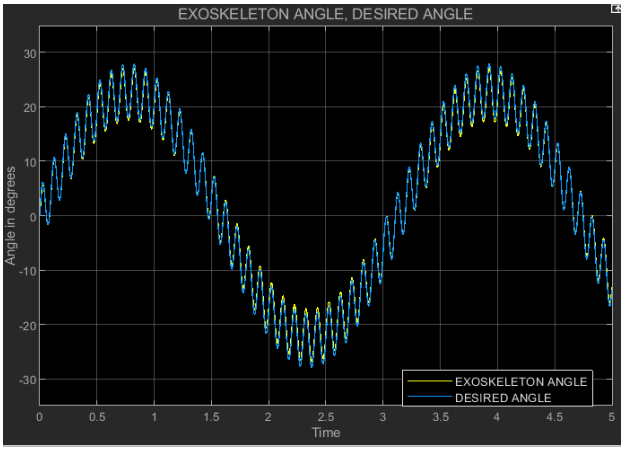

(a) TRACKING RESPONSE : NO LOAD

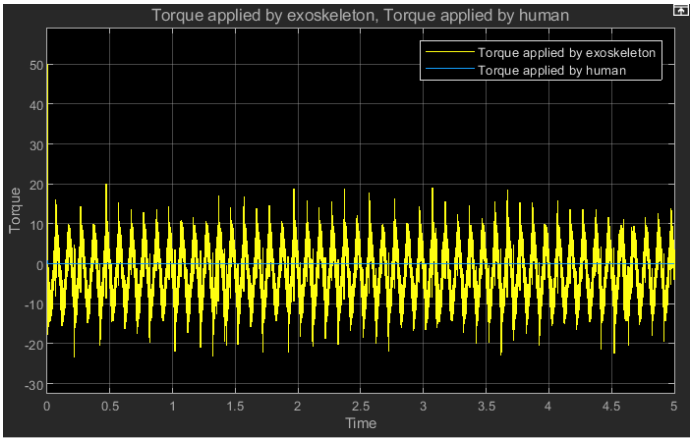

(b) TORQUE PROFILE: NO LOAD

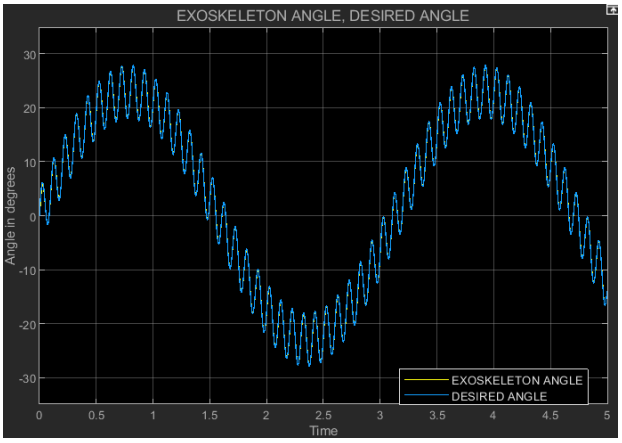

(c) TRACKING RESPONSE : 17 Kg LOAD

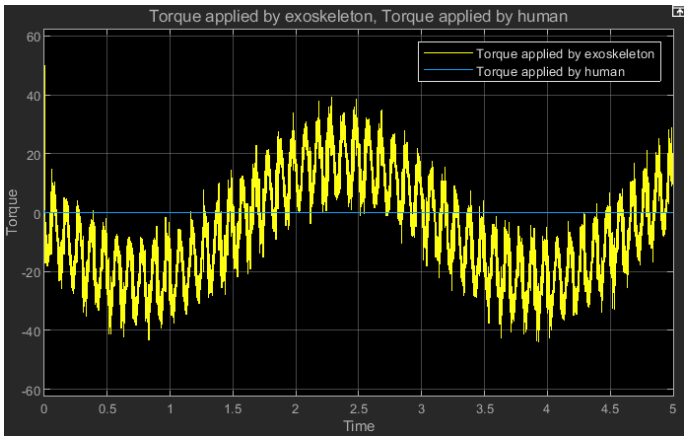

(d) TORQUE PROFILE: 17 Kg LOAD

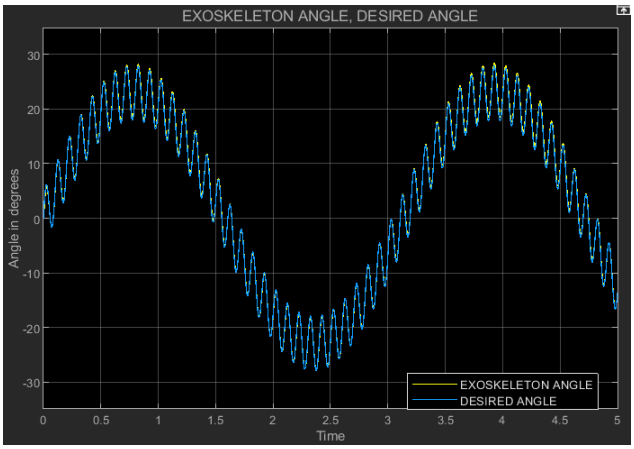

(e) TRACKING RESPONSE : 22.6 Kg LOAD

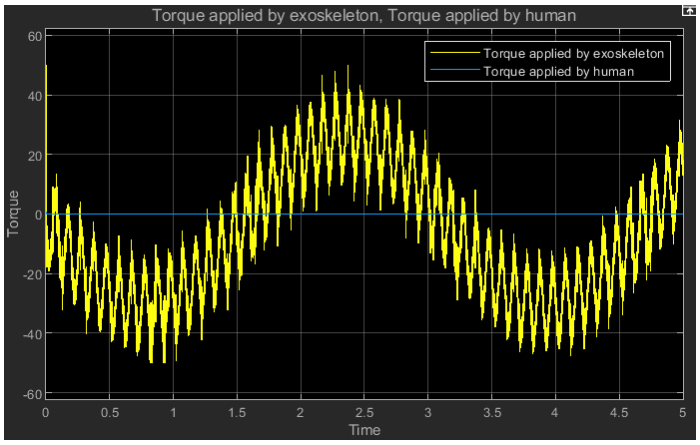

(f) TORQUE PROFILE: 22.6 Kg LOAD

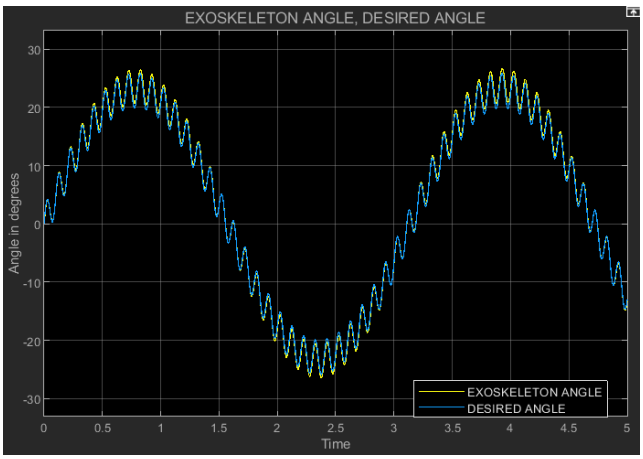

(g) TRACKING RESPONSE : 22.6 Kg LOAD

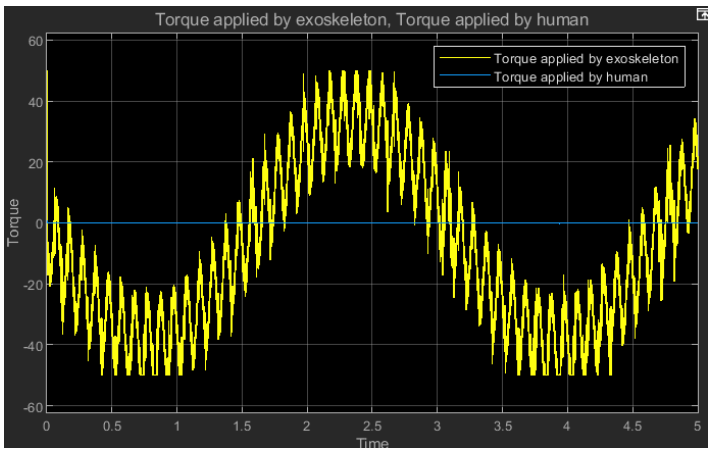

(h) TORQUE PROFILE: 22.6 Kg LOAD

Fig. 16 : TRACKING AND TORQUE OF ELBOW EXOSKELETON IN PRESENCE OF DISTURBANCE

B. LUMBAR/WAIST EXOSKELETON

All the data is taken and compiled in TABLE 20 from previous sections that are useful in designing and simulating the exoskeleton controller.

The data compiled in TABLE 23 is used hence forth for lumbar/waist exoskeleton.

TABLE 23: DATA USED FOR DESIGNING CONTROLLER FOR LUMBAR/WAIST EXOSKELETON

S.No.	PARAMETER	DESCRIPTION	UNITS	VALUE
1	J_{exo_lumbar}	Moment of Inertia of exoskeleton	Kg-m^2	0.12424
2	J_{motor}	Moment of Inertia of motor	Kg-m^2	0.000306
3	M_{motor}	Mass of motor	Kg	0.6
4	M_{exo_lumbar}	Mass of exoskeleton	Kg	1.5
5	L_{exo_lumbar}	Length of exoskeleton link	m	0.5756
6	K_v	Speed/Velocity Constant	V-s/m	0.272
7	K_t	Torque Constant	N-m/A	0.217
8	L	Motor Inductance	H	0.0025
9	R	Motor Resistance	Ω	2.28
10	GR	Gear Ratio	-	580

The maximum error in tracking angle with and without the disturbance signal for all the test cases as that of the experimental GAIT data is compiled in TABLE 24 for lumbar/waist exoskeleton. The error in tracking is well within acceptable limits with good response time.

TABLE 24: MAXIMUM POSITION TRACKING ERROR FOR GA TUNED PARAMETERS OF CONTROLLER - LUMBAR/WAIST EXOSKELETON

	NO DISTURBANCE				EXTERNAL DISTURBANCE			
LOAD	**No Load**	**17 Kg**	**22.6 Kg**	**29 Kg**	**No Load**	**17 Kg**	**22.6 Kg**	**29 Kg**
LUMBAR/WAIST EXOSKELETON: Maximum Error (degrees)	1.151	1.207	1.2394	1.273	1.532	1.475	1.346	1.365

NOTE – The maximum error in angle occurs during the sencond cycle of the sine wave at a time of roughly 2.5 seconds. The error for the first cycle is significantly smaller lying under 1 degree. This scenario will not occur in practical cases usually, however the error is still within acceptable limits. The torqe profile looks has a very high frequency and amplitude as the operating angle i.e. desired angle keeps on changing constantly as the provided input is a sine wave causing such a response which is expected, this however will drop to a constant value with minimal fluctuations if the wearer hold a steady angle.

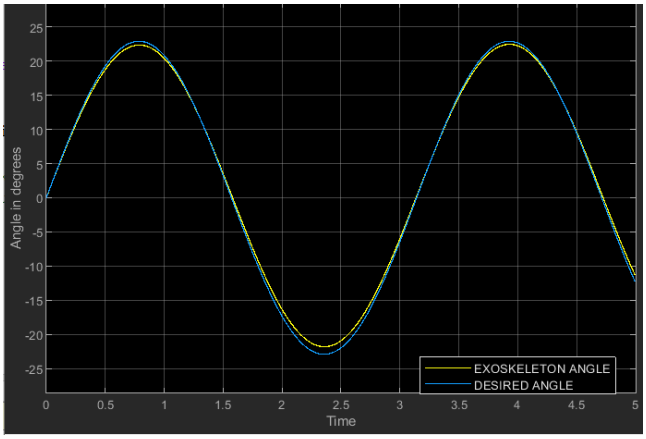

(a) TRACKING RESPONSE : NO LOAD

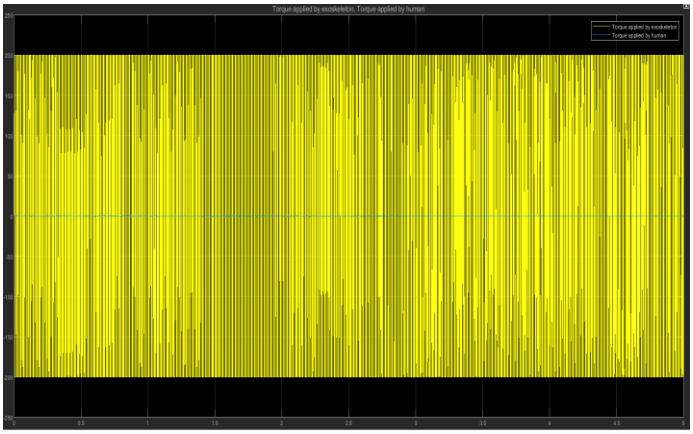

(b) TORQUE PROFILE: NO LOAD

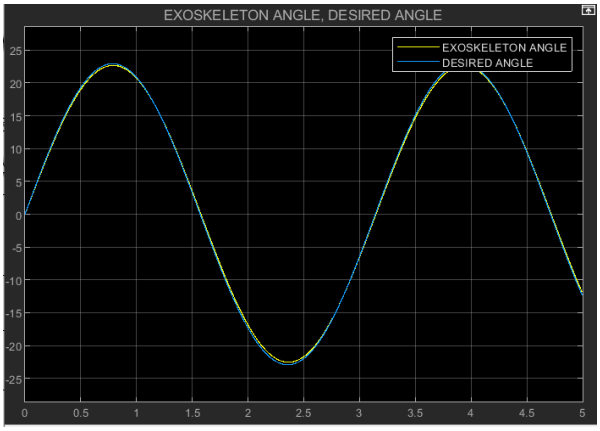

(c) TRACKING RESPONSE : 17 Kg LOAD

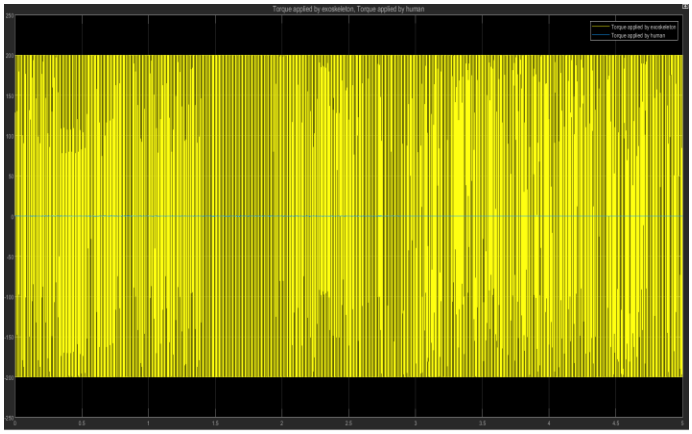

(d) TORQUE PROFILE: 17 Kg LOAD

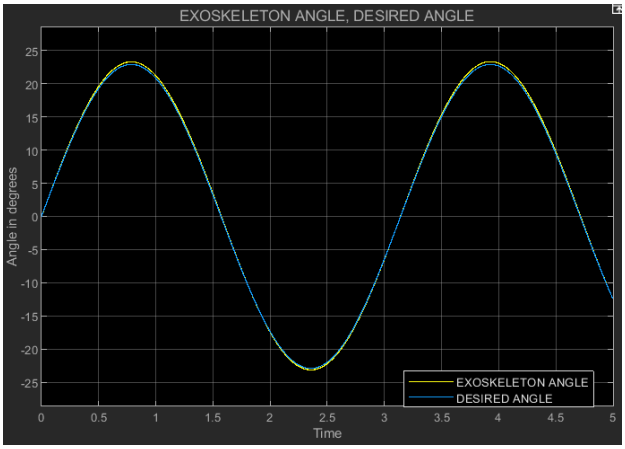

(e) TRACKING RESPONSE : 22.6 Kg LOAD

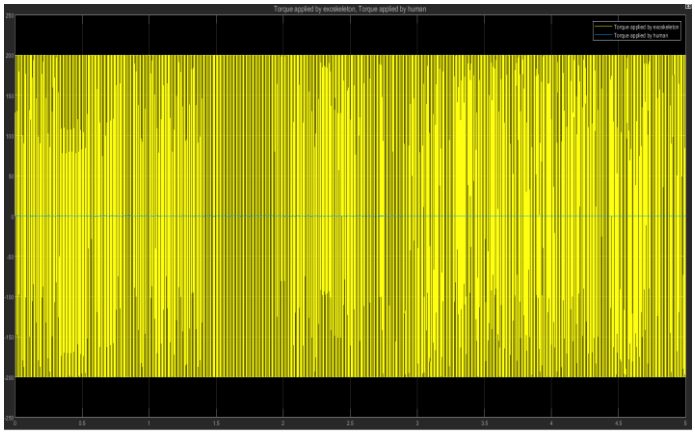

(f) TORQUE PROFILE: 22.6 Kg LOAD

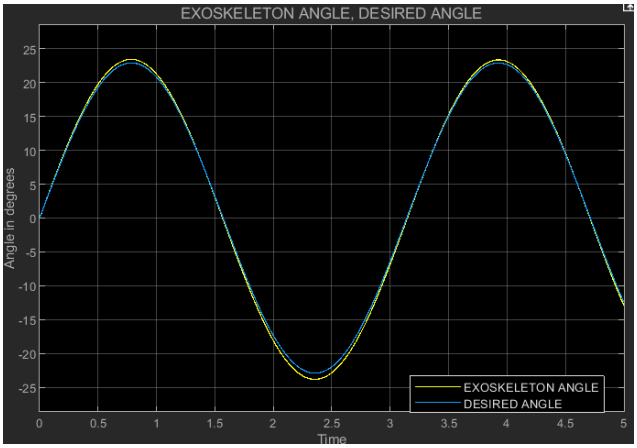

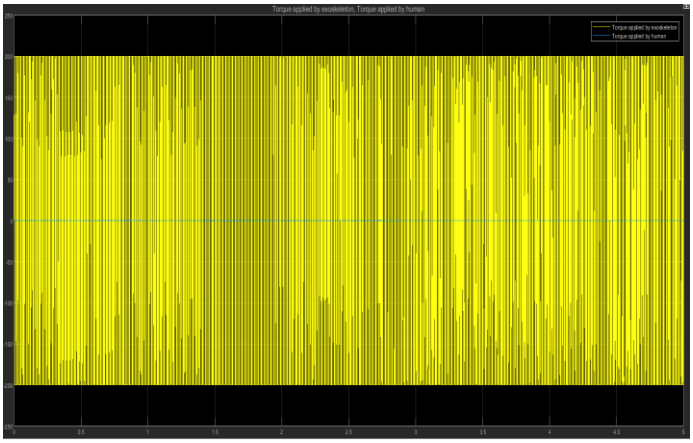

(g) TRACKING RESPONSE : 22.6 Kg LOAD **(h) TORQUE PROFILE: 22.6 Kg LOAD**

Fig. 17 : TRACKING AND TORQUE OF ELBOW EXOSKELETON IN ABSENCE OF DISTURBANCE

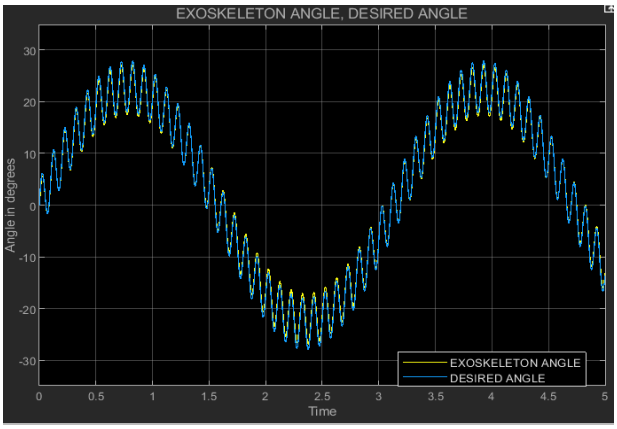

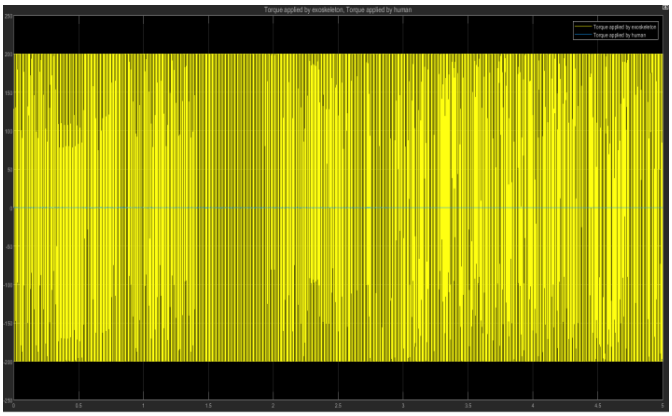

(a) TRACKING RESPONSE : NO LOAD **(b) TORQUE PROFILE: NO LOAD**

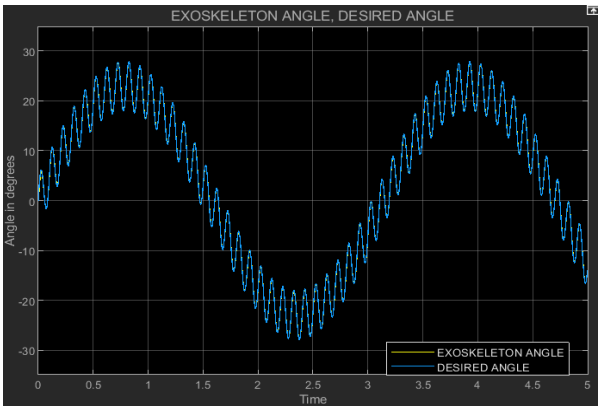

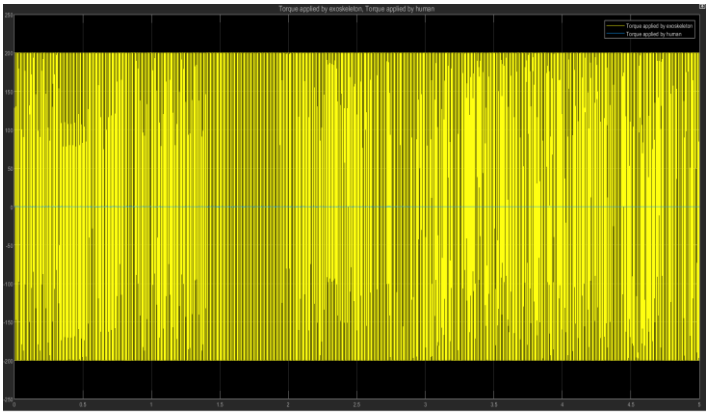

(c) TRACKING RESPONSE : 17 Kg LOAD **(d) TORQUE PROFILE: 17 Kg LOAD**

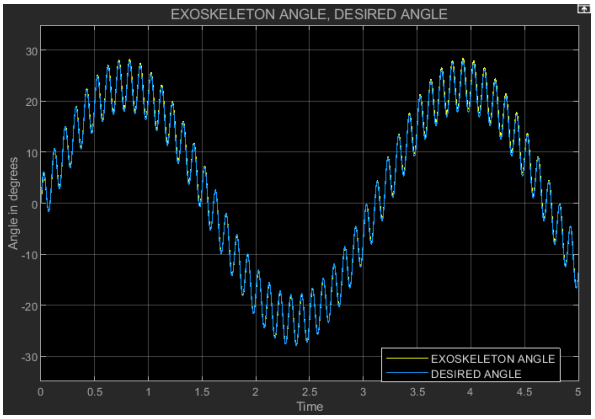

(e) TRACKING RESPONSE : 22.6 Kg LOAD

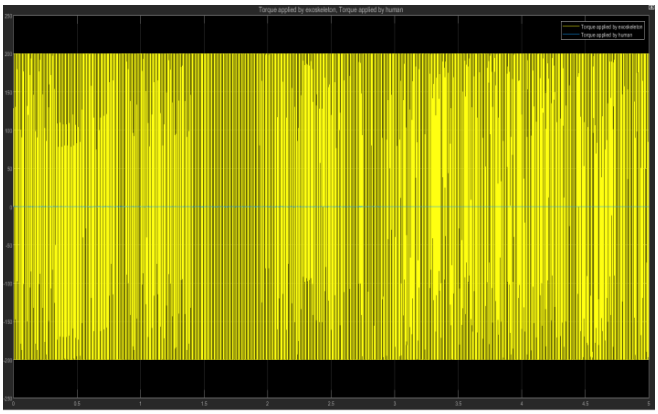

(f) TORQUE PROFILE: 22.6 Kg LOAD

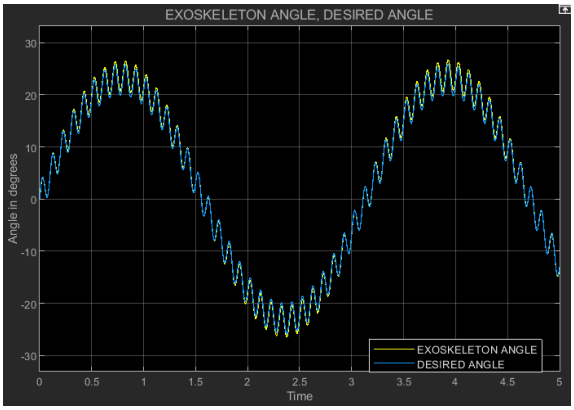

(g) TRACKING RESPONSE : 22.6 Kg LOAD

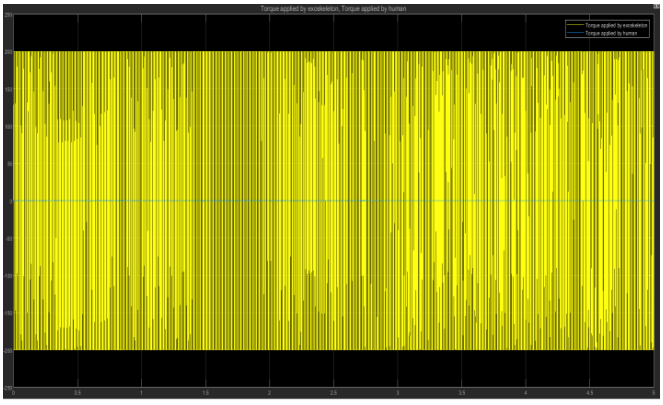

(h) TORQUE PROFILE: 22.6 Kg LOAD

Fig. 18 : TRACKING AND TORQUE OF ELBOW EXOSKELETON IN PRESENCE OF DISTURBANCE

4.5 CONCLUSION AND FUTURE WORK

In the current study elbow and lumbar/waist exoskeleton's electronics and physical design specifications were based on experimental GAIT for a given task at varying speed and varying loads. The physical design concept of the exoskeleton was suggested based on average height and weight of Indian men based on DeLeva's paper[24].

The dynamics equation for 5 DOF full-body exoskeleton and 1 DOF elbow and lumbar/waist exoskeleton model was found using Lagrangian mechanics. The 5 DOF model can also be used to predict the human joint torque without the use of physical sensors as was the case in BLEEX exoskeleton [6].

The dynamic model along with a linear pressure sensor was used while designing the exoskeleton as there is much higher chances of error in case of using a dynamic model to predict the joint torques. The controller model used has 3 PI controller, namely voltage controller, current controller and position controller.

It is particularly difficult to accurately tune multiple PI controllers thus Genetic Algorithm (GA) was coded with multiple objective functions to find global optimum or near global optimum solution to the given elbow and lumbar/waist exoskeleton problem.

The tuned control system gave excellent response even in the presence of external disturbances due to natural tremors that occur in the human body (has higher amplitude at heavier loads and during fatigue). The frequency of the external disturbance/tremors was chosen as 10 Hz (normal human tremor frequency varies from 6-12 Hz) and was modelled as a sine wave of amplitude of 3 degrees.

The work on exoskeleton can be further extended to incorporate other control schemes such as sliding mode-PID, fuzzy logic controller, also neural network self-adaptive PID controller can also be explored and which has the potential to produce excellent controller response but comes at the expense of computation.

The physical design of the exoskeleton can also be studied upon to make the design more flexible such as using a scissor mechanism or flexible link in the lower portion of lumbar/waist exoskeleton, etc.

RFERENCES

1. Yagin, Nicholas. “Apparatus for Facilitating Walking”. U.S. Patent 440,684 filed February 11 1890 and issued November 18, 1890
2. Kelley, C. Leslie. "Pedomotor". U.S. Patent 1,308,675 filed April 24, 1917 and issued July 1, 1919.
3. Mosher, Ralph. “Handyman to Hardiman” (PDF). Cybernetic Zoo.
4. Baldovino, Renann; Jamisola, Rodrigo, Jr. (2017). "A survey in the different designs and control systems of powered-exoskeleton for lower extremities" (PDF). Journal of Mechanical Engineering and Biomechanics, Rational Publication. 1 (4): 103–115. doi:10.24243/JMEB/1.4.192.
5. Sankai, Y., 2011, HAL: Hybrid Assistive Limb Based on Cybernics Robotics Research, M. Kaneko and Y. Nakamura, Editors., Springer Berlin / Heidelberg. p. 25-34
6. Zoss, A.B., H. Kazerooni, and A. Chu, 2006. Biomechanical design of the Berkeley lower extremity exoskeleton (BLEEX), IEEE/ASME Transactions on Mechatronics, vol. 11, no. 2, pp. 128-138.
7. Xinyu Ji & Dashuai Wang & Pengfei Li & Liangsheng Zheng & Jianquan Sun & Xinyu Wu, 2020. "SIAT-WEXv2: A Wearable Exoskeleton for Reducing Lumbar Load during Lifting Tasks," Complexity, Hindawi, vol. 2020, pages 1-12, November.
8. Kim B, Deshpande AD. An upper-body rehabilitation exoskeleton Harmony with an anatomical shoulder mechanism: Design, modeling, control, and performance evaluation. The International Journal of Robotics Research. 2017;36(4):414-435. doi:10.1177/0278364917706743
9. Garrec, P.; Friconneau, J.; Measson, Y.; Perrot, Y. ABLE, an innovative transparent exoskeleton for the upper-limb. In Proceedings of the IEEE/RSJ International Conference on Intelligent Robots and Systems, Nice, France, 22–26 September 2008; pp. 1483–1488
10. Giovacchini F, Vannetti F, Fantozzi M, Cempini M, Cortese M, Parri A, et al. A lightweight active orthosis for hip movement assistance. Robot Auton Syst 2015; 73:123–34.
11. Klein, J.; Spencer, S.; Allington, J.; Bobrow, J.E.; Reinkensmeyer, D.J. Optimization of a parallel shoulder mechanism to achieve a high-force, low-mass, robotic-arm exoskeleton. IEEE Trans. Robot. 2010, 26, 710–715

12. T. Gurriet et al., "Towards Restoring Locomotion for Paraplegics: Realizing Dynamically Stable Walking on Exoskeletons," 2018 IEEE International Conference on Robotics and Automation (ICRA), 2018, pp. 2804-2811, doi: 10.1109/ICRA.2018.8460647.
13. X. Cui, W. Chen, X. Jin and S. K. Agrawal, "Design of a 7-DOF Cable-Driven Arm Exoskeleton (CAREX-7) and a Controller for Dexterous Motion Training or Assistance," in IEEE/ASME Transactions on Mechatronics, vol. 22, no. 1, pp. 161-172, Feb. 2017, doi: 10.1109/TMECH.2016.2618888.
14. Sankai Y. (2010) HAL: Hybrid Assistive Limb Based on Cybernics. In: Kaneko M., Nakamura Y. (eds) Robotics Research. Springer Tracts in Advanced Robotics, vol 66. Springer, Berlin, Heidelberg. https://doi.org/10.1007/978-3-642-14743-2_3
15. H.K. Ko, S.W. Lee, D.H. Koo, I. Lee, D.J. Hyun, Waist-assistive exoskeleton powered by a singular actuation mechanism for prevention of back-injury, Robotics and Autonomous Systems (2018), https://doi.org/10.1016/j.robot.2018.05.008
16. J. F. Veneman, R. Kruidhof, E. E. G. Hekman, R. Ekkelenkamp, E. H. F. Van Asseldonk and H. van der Kooij, "Design and Evaluation of the LOPES Exoskeleton Robot for Interactive Gait Rehabilitation," in IEEE Transactions on Neural Systems and Rehabilitation Engineering, vol. 15, no. 3, pp. 379-386, Sept. 2007, doi: 10.1109/TNSRE.2007.903919.
17. K. H. Low, X. Liu, H. Yu, "Design and Implementation of NTU Wearable Exoskeleton as an Enhancement and Assistive Device", Applied Bionics and Biomechanics, vol. 3, Article ID 701729, 17 pages, 2006. https://doi.org/10.1533/abbi.2006.0030
18. Crea, S.; Cempini, M.; Mazzoleni, S.; Carrozza, M.C.; Posteraro, F.; Vitiello, N. Phase-II clinical validation of a powered exoskeleton for the treatment of elbow spasticity. Front. Neurosci. 2017, 11, 261.
19. Wu Q, Wang X, Du F, Zhang X. Design and Control of a Powered Hip Exoskeleton for Walking Assistance. International Journal of Advanced Robotic Systems. March 2015. doi:10.5772/59757
20. Xinyu Ji, Dashuai Wang, Pengfei Li, Liangsheng Zheng, Jianquan Sun, Xinyu Wu, "SIAT-WEXv2: A Wearable Exoskeleton for Reducing Lumbar Load during Lifting

Tasks", Complexity, vol. 2020, Article
ID 8849427, 12 pages, 2020. https://doi.org/10.1155/2020/8849427

21. Schmidt, and C. J. Walsh, “Soft Exosuit for Hip Assistance,” Robotics and Autonomous Systems (RAS) Special Issue on Wearable Robotics, vol. 73, pp. 102-110, 2015.
22. B. Beigzadeh, M. Ilami and S. Najafian, "Design and development of one degree of freedom upper limb exoskeleton," 2015 3rd RSI International Conference on Robotics and Mechatronics (ICROM), 2015, pp. 223-228, doi: 10.1109/ICRoM.2015.7367788.
23. Schrade, S.O., Dätwyler, K., Stücheli, M. et al. Development of VariLeg, an exoskeleton with variable stiffness actuation: first results and user evaluation from the CYBATHLON 2016. J NeuroEngineering Rehabil 15, 18 (2018). https://doi.org/10.1186/s12984-018-0360-4
24. de Leva P. Adjustments to Zatsiorsky-Seluyanov's segment inertia parameters. J Biomech. 1996 Sep;29(9):1223-30. doi: 10.1016/0021-9290(95)00178-6. PMID: 8872282.
25. Anam, Khairul and Adel Al-Jumaily. “Active Exoskeleton Control Systems: State of the Art.” *Procedia Engineering* 41 (2012): 988-994.
26. Xiuxia, Y., L. Gui, Y. Zhiyong, and G. Wenjin, 2008." Lower Extreme Carrying Exoskeleton Robot Adative Control Using Wavelet Neural Networks," Fourth International Conference on Natural Computation (ICNC).
27. . Nef, T., M. Guidali, and R. Riener, 2009. ARMin III–arm therapy exoskeleton with an ergonomic shoulder actuation, Applied Bionics and Biomechanics, vol. 6, no. 2, pp. 127-142.
28. P. K. Jamwal and S. M. H. Hussain Ghayesh, ‘‘Robotic orthoses for gait rehabilitation: An overview of mechanical design and control strategies,’’ Proc. Inst. Mech. Eng., H, J. Eng. Med., vol. 234, no. 5, pp. 444–457, 2020.
29. Hogan N. (1985). Impedance control - An approach to manipulation. I - Theory. II - Implementation. III - Applications. *ASME Trans. J. Dynam. Syst. Measure. Control B* 107, 1–24. 10.1115/1.3140713
30. Hogan N. (1985). Impedance control - An approach to manipulation. I - Theory. II - Implementation. III - Applications. *ASME Trans. J. Dynam. Syst. Measure. Control B* 107, 1–24. 10.1115/1.3140713

31. Rosen J., Brand M., Fuchs M. B., Arcan M. (2001). A myosignal-based powered exoskeleton system. *IEEE Trans. Syst. Man Cybernet. Part A Syst. Hum.* 31, 210–222. 10.1109/3468.925661

32. Fleischer C., Hommel G. (2008). A human–exoskeleton interface utilizing electromyography. *IEEE Trans. Robot.* 24, 872–882. 10.1109/TRO.2008.926860

33. Comparing neural control and mechanically intrinsic control of powered ankle exoskeletons. *Koller JR, David Remy C, Ferris DP. IEEE Int Conf Rehabil Robot. 2017 Jul; 2017():294-299.*

34. Toxiri S., Koopman A. S., Lazzaroni M., Ortiz J., Power V., de Looze M. P., et al. (2018). Rationale, implementation and evaluation of assistive strategies for an active back-support exoskeleton. *Front. Robot. AI* 5:53 10.3389/frobt.2018.00053

35. Adaptive Control of Exoskeleton Robots for Periodic Assistive Behaviours Based on EMG Feedback Minimisation. *Peternel L, Noda T, Petrič T, Ude A, Morimoto J, Babič J. PLoS One. 2016; 11(2):e0148942.*

36. Li Yang, Xu Cheng, Guan Xiaorong Modeling and simulation study of electromechanically system of the human extremity exoskeleton. Journal of Vibroengineering, Vol. 18, Issue 1, 2016, p. 551-561.

37. Z. Yang, L. Gui, X. Yang, W. Gu and Y. Zhang, "Simulation Research of Exoskeleton Suit Based on Sensitivity Amplification Control," *2007 IEEE International Conference on Automation and Logistics*, 2007, pp. 1353-1357, doi: 10.1109/ICAL.2007.4338780.

38. Nguyen Thang Cao, Parnichkun Manukid, Phan My Thi Tra, Nguyen Anh Dong, Pham Chung Ngoc, Nguyen Hieu Nhu Force control of upper limb exoskeleton to support user movement. Journal of Mechanical Engineering, Automation and Control Systems, Vol. 1, Issue 2, 2020, p. 89-101. https://doi.org/10.21595/jmeacs.2020.21689

39. Li Yang, Xu Cheng, Guan Xiaorong, Li Zhong Optimization of the control scheme for human extremity exoskeleton. Journal of Vibroengineering, Vol. 18, Issue 8, 2016, p. 5432-5439. https://doi.org/10.21595/jve.2016.17397

40. Zhu Q, Mao Y, Xiong R, Wu J. Adaptive Torque and Position Control for a Legged Robot Based on a Series Elastic Actuator. *International Journal of Advanced Robotic Systems*. January 2016. doi:10.5772/62204

41. Kong K, Jeon D. Design and control of an exoskeleton for the elderly and patients. Mechatronics, IEEE/ASME Transactions on. 2006;11(4):428–432.

42. Chen, B., Grazi, L., Lanotte, F., Vitiello, N., and Crea, S. (2018). A real-time lift detection strategy for a hip exoskeleton. *Front. Neurorobot*. 12:17. doi: 10.3389/fnbot.2018.00017

43. Proietti, T.; Crocher, V.; Roby-Brami, A.; Jarrassé, N. Upper-limb robotic exoskeletons for neurorehabilitation: A review on control strategies. IEEE Rev. Biomed. Eng. 2016, 9, 4–14. doi:10.1109/RBME.2016.2552201.